The coupled perturbed electron propagator in the two-particle-hole and extended two-particle-hole Tamm-Dancoff approximations

ARTICLE *in* INTERNATIONAL JOURNAL OF QUANTUM CHEMISTRY · JANUARY 1997

Impact Factor: 1.43 · DOI: 10.1002/(SICI)1097-461X(1997)63:2<483::AID-QUA19>3.0.CO;2-9

2 AUTHORS:

Michael S Deleuze
Hasselt University
132 PUBLICATIONS **2,674** CITATIONS
SEE PROFILE

Barry T Pickup
The University of Sheffield
85 PUBLICATIONS **2,371** CITATIONS
SEE PROFILE

The Coupled Perturbed Electron Propagator in the Two-Particle-Hole and Extended Two-Particle-Hole Tamm–Dancoff Approximations

MICHAEL S. DELEUZE,[1] BARRY T. PICKUP[2]

[1]*Laboratoire de Chimie Théorique Appliquée, Facultés Universitaires Notre-Dame de la Paix, Rue de Bruxelles 61, B5000 Namur, Belgium*

[2]*Department of Chemistry and Centre for Molecular Materials, The University of Sheffield, Sheffield S3 7HF, England*

Received 23 February 1996; revised 24 July 1996; accepted 15 August 1996

ABSTRACT: The equations satisfied by the first-order perturbed electron propagator in an applied external field are examined at a level equivalent to the two-particle–hole Tamm–Dancoff and extended two-particle–hole Tamm–Dancoff approximations (2ph-TDA). These schemes are derived with the intention of evaluating linear and quadratic response properties through second and third order in correlation. Their derivation is based on a combination of the diagrammatic and algebraic superoperator methods. Both schemes account for the polarization of the 2p–1h and 2h–1p responses and bielectron interactions under an external field. The 2ph-TDA scheme is correct up to second order in electronic correlation and includes infinite geometric series of mixed RPA–ladder-type character. Its extended version is derived consistently through third order and accounts for a first-order screening of the external field and bielectron interaction by the effects of electronic correlation. Int J Quant Chem **63**: 483–509, 1997

Key words: linear response; quadratic response; perturbation theory; electronic correlation; Green's function

Introduction

The one-electron propagator [1–3] provides a powerful apparatus [4] for theories of electron ionization and attachment processes in many-electron systems, a subject that was a major interest of Professor Jean-Louis Calais [5]. From this function, one can directly calculate ionization and attachment energies (i.e., vertical energy differences between a reference N-electron ground state and a series of 'excited' $(N \pm 1)$-electron states). It is also possible to obtain the ground-state energy [6] and one-density [7], as well as elastic scattering [8, 9] and photoionization cross sections [4, 10]. The related polarization propagator ap-

Correspondence to: M. S. Deleuze. Present address: c/o Dr. F. Zerbetto, Dipartimento di Chemica "G. Ciamician", Università degli Studi di Bologna, via F. Selmi 2, I40126 Bologna, Italy.

 CCC 0020-7608 / 97 / 020483-27

proach [11] has alternatively been used with considerable success to calculate electronic excitation energies, transition moments, and, thereby, linear response properties. As compared with more conventional configuration interaction treatments of electronic transitions, propagators in general [12] offer the combined advantages of error cancellations in energy differences, systematic compactness in high-order approximations [13], energy separability (size-consistency—the correct behavior with respect to dissociation of a complex system into multiple noninteracting parts [14, 15]), and, finally, the correct scaling [14–18] of the computed transition energies and moments with particle number (size-intensivity) in the thermodynamic limit [1, 19, 20].

The present article considers a different but connected matter. Pickup and co-workers have shown that ground-state molecular linear response tensors [21, 22] can be obtained by considering the properties of the first-order perturbed electron propagator in the presence of an applied external field [23]. In analogy with the coupled perturbed Hartree–Fock (CPHF) scheme [24, 25], the coupled perturbed one-electron propagator (CPEP) approach is an iterative procedure, which considers the perturbed one-electron density obtained from approximate forms of the perturbed one-electron propagator, by means of contour integration in the complex frequency space. As in CPHF theory, the first-order perturbed one-electron density gives thereby access to linear [23] and quadratic [26] molecular responses. As compared with a direct treatment using the polarization propagator, the major advantage of the perturbed electron propagator is that it restricts attention to the perturbed density. As shall be shown, for a comparable treatment with respect to electronic correlation, this approach therefore yields matrix equations of lower dimension, at the expense of losing information on transition energies and moments.

Diagrammatic perturbation theory provides a powerful technique for constructing high-order (resummed or renormalized) theories, as well as a pictorial approach with mechanistic interpretations [27] of ''processes'' which occur on the creation of a hole (ionization) or a particle (attachment) in the correlated N-electron Fermi sea. The superoperator formalism [28] provides an alternative approach to the development of approximations to the one-electron or polarization propagators. This method uses the formal properties of the propagator equations of motion (EOM) [29] to introduce a system of equations which can be simplified using linear algebra methods, i.e., organization into large-dimension secular equations which are familiar from other methods of variational quantum chemistry. The linear spaces involved in the equations are defined in terms of operator spaces [30] constructed around mappings between the N-electron ground state and the $(N \pm 1)$-electron portions of Fock space (taking the electron propagator as an example).

The introduction of linear algebra has algorithmic advantages and leads also rather transparently to the use of techniques of spin and spatial symmetry adaptation to simplify the problem. On the other hand, a derivation of the propagator equations of motion using [31, 32] the algebraic superoperator approach may imply a tedious and difficult task, namely, the expansion of binary products using anticommutation relationships. Since both diagrams and superoperator methods lead to the same set of approximations, it is often worthwhile to bypass this step by means of diagrammatic tools. For instance, specific approximations to the one-electron propagator have been derived consistently up to fourth order in the correlation potential using the so-called algebraic diagrammatic construction (ADC) procedure, based on a comparison [33–36] of the linear matrix equations needed to expand the propagator with the related diagrammatic perturbation series. Along the same lines, a consistent second-order expansion of the polarization propagator (SOPPA), originally derived [37] using the EOM formalism, was later recast [38] in ADC form.

It is well known that rather high-order theories are required for a quantitative treatment of inner- and outer-valence ionization processes. Indeed, it is often considered that the two-particle-hole Tamm–Dancoff approximation (2ph-TDA) [33, 39] is the lowest order of theory which can be considered to give a reliable description of the pole positions and strengths for a wide range of molecules [4]. 2ph-TDA is a theory based on a Hartree–Fock (HF) reference ground state, which is correct up to second order in electron correction and contains partial higher-order series, so it is necessarily expensive. For accuracy, however, it is often necessary to consider an extended third-order version [35] of this scheme, including correlation corrections to the reference ground state. Along the same lines, it is usually considered that a

consistent treatment of excitation spectra and linear responses requires at least a full second-order expansion (SOPPA) of the polarization propagator, although it is sometime claimed [40] that accurate excitation energies, differing from experiment by less than 0.2 eV, could be obtained only at the next order of approximation. To date, however, no third-order scheme (TOPPA) has ever been explicitly derived for the polarization propagator.

Up to the present, only equations which account for a strict second-order expansion in correlation have been presented [23, 41] for the coupled perturbed electron propagator. As shown by a few numerical tests, this accounts for a calculation of linear and quadratic responses at the MP2 level. The purpose of this article is to derive a 2ph-TDA and extended 2ph-TDA versions of the coupled perturbed electron propagator, with the aim of evaluating response properties at a level comparable to SOPPA and TOPPA, respectively. In the next section, we first outline the properties of the exact one-electron propagator $\mathbf{G}_1(\omega)$ and the related self-energy $\mathbf{\Sigma}(\omega)$, as obtained from an expansion using the algebraic superoperator approach. As a byproduct, we also provide in this section the very first complete derivation of the 2ph-TDA scheme within the algebraic superoperator approach, considering a nonorthogonal $\{h_3, h_5\}$ operator manifold. In the third section, these considerations are extended to the case of a molecule perturbed under an external field. In this section, we focus on the analytical properties of a first-order perturbed form $\mathbf{G}_1^{(1)}(\omega)$ of the electron propagator and its relationships with the perturbed one-electron density $\boldsymbol{\rho}_1^{(1)}$. An exact form of the perturbed self-energy $\mathbf{\Sigma}^{(1)}(\omega)$ is derived in the fourth section. From its analytical properties, we eventually derive a set of systematic approximations for $\mathbf{\Sigma}^{(1)}(\omega)$, which represent infinite partial summations in topological series of Feynman diagrams. Specifically, the 2ph-TDA and extended 2ph-TDA schemes recover renormalized forms of $\mathbf{\Sigma}^{(1)}(\omega)$ being exact through second and third order in correlation, respectively.

As for the unperturbed self-energy [3, 4, 33], this derivation implies the evaluation of all time-ordered Feynman diagrams accounting for the second-order and third-order perturbed self-energies at the next order of approximation and the extraction from these diagrams of the matrix blocks to which they relate. This represents a considerable task, since the number of terms to be considered in this case is comparable to that found for a third- and fourth-order expansion of the unperturbed self-energy. As will be shown in the fifth and sixth sections, a perturbation expansion in terms of Feynman diagrams involves, in fact, many combinations over a rather limited number of substructures. By means of appropriate tools [14], it can then be reformulated diagrammatically in a very compact form, which enables some physical insight and a straightforward expansion of the required block matrices.

The Electron Propagator

The electron propagator is defined [12] as a causal two-time propagator in the resolvent form and the energy representation as

$$G_{1qp} = \langle \Psi_0^N | \Big\{ a_q (\omega + E_0^N - H + i\varepsilon)^{-1} a_p^+ + a_p^+ (\omega - E_0^N + H - i\varepsilon)^{-1} a_q \Big\} | \Psi_0^N \rangle, \quad (1)$$

which is the starting point of our work. The propagator is a matrix indexed by a set of creation and destruction operators $\{a_p^+, a_p\}$ which refer to a complete (formally) orthonormal orbital basis $\{\psi_p\}$. In the present work, this basis is the truncated set of canonical MOs obtained from an SCF calculation on the ground state. The infinitesimal convergence factors ε above are introduced merely to ensure analyticity in appropriate parts of the complex plane. The introduction of a complete set of Fock space states inside the resolvents leads to the Lehmann spectral form

$$G_{1qp} = \sum_a \frac{b_{qa} b_{pa}^*}{\omega + E_0^N - E_a^{N+1} + i\varepsilon} + \sum_i \frac{b_{qi} b_{pi}^*}{\omega - E_0^N + E_i^{N-1} - i\varepsilon}, \quad (2)$$

which includes only $(N \pm 1)$-electron states because of the nature of the Fermi creation and destruction operators. The electron propagator, therefore, has single (first-order) poles at the exact vertical ionization and attachment energies. The numerators in (2) are the Dyson orbital coefficients

$$\begin{aligned} b_{qa} &= \langle \Psi_0^N | a_q | \Psi_a^{N+1} \rangle \\ b_{qi} &= \langle {}_i^N \quad | a_q | \Psi_0^N \rangle. \end{aligned} \quad (3)$$

The propagator equations of motion are obtained by expanding the resolvents in (1) as a series in inverse powers of the energy ω, neglecting the convergence factors. We introduce the Hamiltonian superoperator and its powers, which are defined by their action on an arbitrary operator X as

$$\begin{aligned} \hat{H}X &= [\,X, H\,]_-; \\ \hat{H}^2X &= [\,\hat{X}X, H\,]_- = [[\,X, H\,]_-, H\,]_-; \quad \ldots, \end{aligned} \tag{4}$$

together with the commutators and anticommutators

$$\begin{aligned} [\,X, Y\,]_- &= XY - YX \\ [\,A, B\,]_+ &= AB + BA. \end{aligned} \tag{5}$$

Defining the unit superoperator via

$$\hat{1}\,X = X, \tag{6}$$

we can reexpress the momentum expansion of the resolvent form (1) as

$$G_{1qp} = \langle \Psi_0^N | \left[a_p^+, (\omega\hat{1} - \hat{H})^{-1} a_q \right]_+ | \Psi_0^N \rangle, \tag{7}$$

which is the superoperator resolvent form of the propagator. Superoperators are defined in (4, 6) by their action on arbitrary operators. We look for an analogy with standard quantum mechanics, where one has operators acting on a space of appropriately defined functions, metricized by a scalar product. We define a binary product

$$(\,X|Y\,) = \langle \Psi_0^N | [\,X^+, Y\,]_+ | \Psi_0^N \rangle. \tag{8}$$

This notation enables us to reformat (7) as

$$G_{1qp} = \left(a_p | (\omega\hat{1} - \hat{H})^{-1} | a_q \right). \tag{9}$$

The superoperator resolvent can be replaced by a matrix inverse by introducing a suitable operator manifold $h = (h_1, h_2, \ldots, h_M)$ of dimension M and the so-called inner projection [42, 43]

$$(\omega\hat{1} - \hat{H})^{-1} \cong |h)(h|\omega\hat{1} - \hat{H}|h)^{-1}(h|, \tag{10}$$

which implies that

$$G_{1qp} \cong (a_p|h)(h|\omega\hat{1} - \hat{H}|h)^{-1}(h|a_q). \tag{11}$$

The matrix inverse in (11) is an M-dimensional matrix. With the use of a complete (infinite) operator manifold [30] in (11), one is able to reproduce the exact propagator [28]. The complete manifold [30] h is divided into

$$h = (a_1, g), \tag{12}$$

where $a \equiv a_1 = \{a_p\}$, the set of destruction operators is the a_1 basis, and the complementary basis

$$g = (a_3, a_5, \ldots) \tag{13}$$

comprises subsets defined in terms of the total numbers of creation and destruction operators involved. For example, the a_3 basis is

$$a_3 = \begin{cases} a_a^+ a_i a_j & \forall \quad a, i > j \\ a_i^+ a_a a_b & \forall \quad i, a > b, \end{cases} \tag{14}$$

where we have adopted the convention that MOs labeled $i, j, k, \ldots$ are occupied and those labelled $a, b, c, \ldots$ are unoccupied with respect to the HF ground state. The a_3 basis (and its higher analogs) are designed to map the ground-state HF determinant into the $(N \pm 1)$-electron determinants of successively higher excitation rank so as to span the slices of Fock space needed for a correct representation of all the states embedded in (2). For operator subsets of fermion character, the binary product (8) in the superoperator notation is defined as an expectation value of an anticommutator over a representation of the ground state which is formally exact. It is known that the use of a formally exact operator manifold with an approximate ground-state representation would produce the correct poles but the wrong pole strengths. In practice, the operator manifold has to be truncated, and, simultaneously, the ground state approximated. The operator basis described above is orthonormal with respect to a metric defined on the HF ground state. More generally, it is better to introduce a new operator basis which is Schmidt orthogonalized to the a_1 basis, viz.,

$$b = g - a_1(a_1|g), \tag{15}$$

which has the property

$$(a_1|b) = 0. \tag{16}$$

Using the inner production formula (11) and the new operator basis, we obtain

$$\mathbf{G}_1 = \begin{bmatrix} \mathbf{1}^{aa} & \mathbf{0}^{ab} \end{bmatrix} \begin{bmatrix} \omega\mathbf{1}^{aa} - \mathbf{H}^{aa} & -\mathbf{H}^{ab} \\ -\mathbf{H}^{ba} & \omega\mathbf{S}^{bb} - \mathbf{H}^{bb} \end{bmatrix}^{-1} \times \begin{bmatrix} \mathbf{1}^{aa} \\ \mathbf{0}^{ba} \end{bmatrix}, \quad (17)$$

which is formally exact. The various matrix components in (17) are

$$\mathbf{H}^{xy} = (x|[\,y, H\,]_-) = \mathbf{H}^{yx\dagger}$$
$$\mathbf{S}^{xy} = (x|y). \quad (18)$$

Formula (17) can be simplified using block inversion to give

$$\mathbf{G}_1^{-1}(\omega) = \omega\mathbf{1}^{aa} - \mathbf{H}^{aa} - \mathbf{H}^{bb}(\omega\mathbf{S}^{bb} - \mathbf{H}^{bb})^{-1}\mathbf{H}^{ba}, \quad (19)$$

which is an exact expression.

The simplification of the matrix elements appearing in (17) and (19) will be carried out later, using the Fermi anticommutation rules and the formula for the second quantized Hamiltonian,

$$\hat{H}a_p = [\,a_p, H\,]_- = \sum_q h_{pq}a_q + \frac{1}{2}\sum_{qrs}\langle\, pr||qs\rangle a_r^+ a_s a_q, \quad (20)$$

where the double-bar integral is an antisymmetrized two-electron integral. The final term of (20) includes operators that look very like the a_3 operators of (14), except that the index range involves all triple rank products, not just the 2-hole−1-particle (2h−1p), and 2-particle−1-hole (2p−1h) operators of (14). To avoid linear dependencies, it is therefore useful to define a set of b_3 operators:

$$b_{pqr} = a_p^+ a_q a_r - (1 - P_{qr})a_r\rho_{1qp}, \quad (21)$$

which have been Schmidt-orthogonalized to the operator basis a_1. Equation (21) involves the operator P_{qr} which transposes subscripts. The exact one-density is defined as

$$\rho_{1sr} = \langle \Psi_0^N | a_r^+ a_s | \Psi_0^N \rangle. \quad (22)$$

We can rewrite (20) using the definition (21) as

$$\hat{H}a_p = \sum_q F_{pq}(\boldsymbol{\rho}_1)q_q + \frac{1}{2}\sum_{qrs}\langle\, pr||qs\rangle b_{rsq}, \quad (23)$$

where we have introduced the Fock operator

$$F_{pq}(\boldsymbol{\rho}_1) = h_{pq} + \sum_{rs}\langle\, pr||qr\rangle\rho_{1sr}, \quad (24)$$

defined in terms of the exact ground-state 1-density. The justification of the use of a subset of b_3 operators is via Eq. (23), in that the application of the Hamiltonian superoperator on the a_1 produces just that subset of the full b-space. It follows immediately that

$$H_{pq}^{aa} = \left(a_p|\hat{H}a_q\right) = F(\boldsymbol{\rho}_1)_{pq}$$
$$H_{q'r's',\,p}^{bb} = \left(b_{q'r's'}|\hat{H}a_p\right) = \sum_{qrs}\langle\, pq||sr\rangle S_{q'r's',\,qrs}^{bb}. \quad (25)$$

The overlap matrix elements are obtained also using the anticommutation rules, i.e., basically using Wick's theorem [44] defined for the true vacuum, as

$$S_{q'r's',\,qrs}^{bb} = \left(b_{q'r's'}|b_{qrs}\right) = \delta_{qq'}\rho_{2srs'r'} + (1 - P_{rs}) \times \left[\,\delta_{rr'}\delta_{ss'}\rho_{1q'q} + (1 - P_{rs})\delta_{ss'} \times (\,\rho_{2rq'qr'} - \rho_{1rq}\rho_{1q'r'})\right]. \quad (26)$$

The matrix elements are expressed in terms of the one-body density (22), and the two-body density:

$$\rho_{2rsr's'} = \langle \Psi_0^N | a_r^+ a_{s'}^+ a_s a_r | \Psi_0^N \rangle. \quad (27)$$

The derivation of $\mathbf{H}^{bb}$ matrix elements in a general form equivalent to (25) is a rather complicated procedure. The principles, however, are rather simple to understand. One needs to examine the effect of the Hamiltonian superoperator on the b_3 operators defined in Eq. (21):

$$\hat{H}b_{pqr} = [\,b_{pqr}, H\,]_-. \quad (28)$$

The commutators can be simplified using the fundamental Fermi anticommutation relations. Just as $\hat{H}$ maps the space of a_1 operators into itself and the orthogonalized b_3 space, so is the b_3 space itself mapped into a combination of a_1, b_3, and b_5. The latter is a Schmidt-orthogonalized version of operators based on an $a_p^+ a_q^+ a_r a_s a_t$ structure. Hence,

one can derive equations of the form

$$\hat{H}b_{pqr} = \sum_s a_s B_{s,pqr} + \frac{1}{2}\sum_{stu} b_{stu} B_{stu,pqr} + \frac{1}{12}\sum_{stuvw} b_{stuvw} B_{stuvw,pqr}, \quad (29)$$

where, by construction, the b_5 operators satisfy

$$\begin{aligned}(b_3|b_5) &= 0\\ (a_1|b_5) &= 0.\end{aligned} \quad (30)$$

One can actually deduce that

$$\begin{aligned}H^{bb}_{p'q'r',pqr} &= \left(b_{p'q'r'}|\hat{H}b_{pqr}\right)\\ &= \frac{1}{2}\sum_{stu} S_{p'q'r',stu} B_{stu,pqr}.\end{aligned} \quad (31)$$

After considerable effort, it can be shown that

$$\begin{aligned}B_{stu,pqr} = 2\mathscr{A}_{qr}\mathscr{A}_{tu}\Big\{&2\delta_{sp}\delta_{qt}h_{ru} - h_{sp}\delta_{ru}\delta_{qt}\\ &+ \frac{1}{2}\delta_{sp}\langle rq||ut\rangle\Big\}\\ &+ \sum_{s't'u'v'w'}\delta_{qw'}\Big\{\delta_{pt'}\langle rs'||v'u'\rangle\\ &+ \frac{1}{2}\langle s't'||pu'\rangle\delta_{rv'}\Big\}\\ &\times \Delta_{s't'u'v'w',stu} - 2\mathscr{A}_{qr}\langle rs||ut\rangle\rho_{1qp},\end{aligned} \quad (32)$$

where

$$\begin{aligned}\Delta_{s't'u'v'w',stu} &= \mathscr{A}_{s't'}\mathscr{A}_{u'v'w'}\mathscr{A}_{tu}\\ &\times\{2\delta_{s's}\rho_{3w'v'u',utt'} + 6\delta_{uw'}\gamma_{sv'u'ts't'}\}.\end{aligned} \quad (33)$$

Equations (32) and (33) contain references to the index antisymmetrizers:

$$\mathscr{A}_{p_1p_2\cdots p_n} = \frac{1}{n!}\sum_P \epsilon^P P, \quad (34)$$

where the quantities P are the $n!$ permutations of the indices. The antisymmetrizers ensure that the expressions are fully antisymmetric in terms of the indices involved. This arises because of the Fermi anticommutation properties of creation and destruction operators. The three-body densities appearing in Eq. (33) are defined as

$$\begin{aligned}\rho_{3w'v'u',utt'} &= \langle\Psi_0^N|a'^+_w a'^+_v a'^+_u a_{t'}a_t a_u|\Psi_0^N\rangle\\ \gamma_{sv'u'ts't'} &= \mathscr{A}_{u'v'}[\,\rho_{3sv'u'ts't'} + \delta_{v't}\rho_{2su's't'}].\end{aligned} \quad (35)$$

Equations (23)–(35) are all defined for the exact N-electron ground state and form the basis for a consistent order-by-order expansion in terms of the correlation potential. At zeroth order in such an expansion, one uses HF expectation values. In terms of HF reference states, the densities become

$$\begin{aligned}\rho^{HF}_{1rs} &= \delta_{rs}n_r\\ \rho^{HF}_{2rss'r'} &= (\delta_{ss'}\delta_{rr'} - \delta_{sr'}\delta_{r's})n_r n_s,\end{aligned} \quad (36)$$

with the occupancy indices

$$n_r = \begin{cases}1 & \text{r} \in \text{occ}\\ 0 & \text{r} \in \text{virt.}\end{cases} \quad (37)$$

It is also useful, for later use, to define the complementary index

$$\bar{n}_r = 1 - n_r. \quad (38)$$

The $\mathbf{H}^{aa}$ matrix in the HF limit becomes just a diagonal matrix of orbital energies:

$$H^{aa}_{pq}|^{HF} = \varepsilon_p\delta_{pq}. \quad (39)$$

The $\mathbf{S}^{bb}$ matrix reverts to

$$\begin{aligned}S^{bb}_{q'r's',qrs}\Big|^{HF} &= \delta_{q'q}(1 - P_{rs})\delta_{rr'}\delta_{ss'}\\ &\times\left(n_q\bar{n}_r\bar{n}_s + \bar{n}_q n_r n_s\right),\end{aligned} \quad (40)$$

which is a diagonal matrix which projects just into the 2-hole–1-particle (2h–1p) and 2-particle–1-hole (2p–1h) parts of the operator space, as it should. The HF version of the $\mathbf{H}^{ba}$ and $\mathbf{H}^{bb}$ matrices is, therefore,

$$\begin{aligned}H^{ba[1]}_{aij,p} &= \langle pa||ij\rangle\\ H^{ba[1]}_{iab,p} &= \langle pi||ab\rangle\end{aligned} \quad (41)$$

and

$$\begin{aligned}H^{bb[1]}_{aij,a'i'j'} &= \delta_{aa'}\delta_{ii'}\delta_{jj'}(\varepsilon_i + \varepsilon_j - \varepsilon_a)\\ &- \frac{1}{2}\delta_{aa'}\langle ij||i'j'\rangle + \delta_{ii'}\langle aj'||a'j\rangle\\ &+ \delta_{jj'}\langle ai'||a'i\rangle\end{aligned}$$

$$H^{bb[1]}_{iab,i'a'b'} = \delta_{ii'}\delta_{aa'}\delta_{bb'}(\varepsilon_a + \varepsilon_b - \varepsilon_i) + \frac{1}{2}\delta_{ii'}\langle ab||a'b'\rangle - \delta_{aa'}\langle ib'||i'b\rangle - \delta_{bb'}\langle ia'||i'a\rangle, \quad (42)$$

where the index under square brackets indicates the order attained with respect to correlation.

Returning to Eq. (19), one can expand the exact propagator $\mathbf{G}_1$ from its HF approximation, using

$$\mathbf{G}(\omega) = [\,\omega\mathbf{1} - \boldsymbol{\epsilon} - \boldsymbol{\Sigma}(\omega)]^{-1}, \quad (43)$$

where $\boldsymbol{\epsilon}$ is the diagonal matrix of orbital energies resulting from (39) and the self-energy matrix can be divided into two kinds of terms

$$\boldsymbol{\Sigma}(\omega) = \boldsymbol{\Sigma}(\infty) + \mathbf{M}(\omega). \quad (44)$$

In (44), the irreducible dynamic self-energy term

$$\mathbf{M}(\omega) = \mathbf{H}^{ab}(\omega\mathbf{S}^{bb} - \mathbf{H}^{bb})^{-1}\mathbf{H}^{ba} \quad (45)$$

contains all terms strictly depending on the frequency ω. In this equation, the ''constant'' part of the self-energy,

$$\boldsymbol{\Sigma}(\infty) = \mathbf{F}(\boldsymbol{\rho}_1^{[corr]})$$
$$\boldsymbol{\Sigma}_{pq}(\infty) = \sum_{rs}\langle pr||qs\rangle\rho^{[corr]}_{1sr}, \quad (46)$$

was obtained by expanding the exact one-density in the expressions for $\mathbf{H}^{aa}$ displayed in Eq. (24),

$$\boldsymbol{\rho}_1 = \boldsymbol{\rho}_1^{[HF]} + \boldsymbol{\rho}_1^{[corr]}, \quad (47)$$

in terms of a ''zeroth-order'' HF term with a correction arising from the effects of electron correlation. The constant part of the self-energy is named $\boldsymbol{\Sigma}(\infty)$ because

$$\lim_{\omega\to\infty}\boldsymbol{\Sigma}(\omega) = \boldsymbol{\Sigma}(\infty), \quad (48)$$

since $\mathbf{M}(\omega) \cong O(1/\omega)$. The whole self-energy matrix can be viewed as a renormalization correction to the HF propagator:

$$\mathbf{G}_1^{HF} = (\omega\mathbf{1} - \boldsymbol{\epsilon})^{-1} \quad (49)$$

The self-energy accounts for the effects of electron correlation during ionization and attachment processes. The terms surviving in the self-energy as $\boldsymbol{\Sigma}(\infty)$ represent correlation effects which occur on a short time scale, i.e., instantaneously. The remaining ''dynamic'' effects from $\mathbf{M}(\omega)$ occur on time scales linked reciprocally to the frequency (energy in a.u.) involved. Using many-body perturbation theory, it is easy to show that $\boldsymbol{\rho}_1^{[corr]}$ leads off at second order in electron correlation—a fact which ensures that $\boldsymbol{\Sigma}(\infty)$ is at least of third order. The lowest-order correction of $\mathbf{G}_1^{HF}$ comes, in fact, from $\mathbf{M}(\omega)$ at second order.

From (45), it is obvious that the dynamic self-energy $\mathbf{M}(\omega)$ has the same analytical structure as the exact propagator, i.e., it yields only first-order (single) poles in terms of the Laurent expansion. At this point, it is useful to remember that a direct inclusion of third-order self-energy diagrams would destroy this analytical structure, since some of these terms display a ω^{-2} dependence. The 2ph-TDA expansion was precisely introduced in [33] as a structure invariant renormalization [45] of $\mathbf{M}(\omega)$.

For the purpose of a perturbation expansion of the one-electron propagator in powers of an external field, it is more convenient to recombine the HF and the correlation parts of the electron density and rewrite from Eqs. (43), (44), and (46) the unperturbed propagator as

$$\mathbf{G}(\omega) = (\omega\mathbf{1} - \mathbf{F}(\boldsymbol{\rho}_1) - \mathbf{M}(\omega))^{-1}, \quad (50)$$

where the one-density upon which the Fock operator depends in (50) is the *exact* one-density of (22).

The Perturbed Electron Propagator

The concept of the perturbed propagator arises from the connection between the electron propagator and the one-density via the Coulson contour [46], which encloses just the ionization sector. Hence, by integrating the resolvent form of Eq. (1) over this contour $\mathscr{C}$, we see that

$$\frac{1}{2\pi i}\oint_c d\omega G_{qp}(\omega) = \sum_i b_{qi}b^*_{pi} = \sum_i \langle\Psi_0^N|a_p^+|\Psi_i^{N-1}\rangle\langle\Psi_i^{N-1}|a_q|\Psi_0^N\rangle = \langle\Psi_0^N|a_p^+a_q|\Psi_0^N\rangle = \rho_{1qp}. \quad (51)$$

We now suppose that the electron density is perturbed in the presence of an applied static one-electron external potential $h^{(1)}$. The many-body Hamiltonian can then be written as

$$H = H^{(0)} + h^{(1)}, \quad (52)$$

where the upper-case notation for the perturbation is meant to emphasize the fact that the perturbations of interest are all of the form of one-electron operators. We can make a formal expansion of the one-density order by order in the *applied potential*:

$$\boldsymbol{\rho}_1 = \boldsymbol{\rho}_1^{(0)} + \boldsymbol{\rho}_1^{(1)} + \cdots, \tag{53}$$

where the index under the parentheses gives the order attained with respect to the external field.

It is important to distinguish, at all times, the external applied potential from a many-body perturbation expansion in terms of electron correlation; they are two distinct perturbations: The external potential is the perturbation involved in the molecular response which is the subject to this article. The correlation potential is an internal perturbation which is used as part of the apparatus of many-body theory to generate high-order approximations to the quantities of interest.

It follows from (53) that it should also be possible to expand the quantities appearing in expressions (50):

$$\begin{aligned} \mathbf{F} &= \mathbf{F}^{(0)} + \mathbf{F}^{(1)} + \mathbf{F}^{(2)} + \cdots \\ \mathbf{M}(\omega) &= \mathbf{M}^{(0)}(\omega) + \mathbf{M}^{(1)}(\omega) + \mathbf{M}^{(2)}(\omega) + \cdots \\ \mathbf{G}_1(\omega) &= \mathbf{G}_1^{(0)}(\omega) + \mathbf{G}_1^{(1)}(\omega) + \mathbf{G}_1^{(2)}(\omega) + \cdots, \end{aligned} \tag{54}$$

in exactly the same way. Using (50), it is easy to identify the first order perturbed propagator (in the external field):

$$\mathbf{G}_1^{(1)} = \mathbf{G}_1^{(0)}(\mathbf{F}^{(1)} + \mathbf{M}^{(1)})\mathbf{G}_1^{(0)}. \tag{55}$$

It is also obvious that

$$\boldsymbol{\rho}_1^{(1)} = \frac{1}{2\pi i}\oint_C d\omega\, \mathbf{G}_1^{(1)}(\omega), \tag{56}$$

so that (56) generates an iterative scheme for determining the perturbed density, provided that one can fully evaluate the quantities appearing in (55). Indeed, by neglecting the contribution arising from $\mathbf{M}^{(1)}$, it is very easy to show that Eqs. (55) and (56) are identical to the familiar CPHF scheme [24, 25].

We now consider the analytic properties of the first-order perturbed electron propagator. We consider the spectral resolution formula (1) and expand in powers of the external field the Dyson orbital coefficients:

$$\begin{aligned} b_{pi} &= b_{pi}^{(0)} + b_{pi}^{(1)} + \cdots \\ b_{pa} &= b_{pa}^{(0)} + b_{pa}^{(1)} + \cdots, \end{aligned} \tag{57}$$

and the state energies:

$$\begin{aligned} E_0^N &= E_0^{N(0)} + E_0^{N(1)} + \cdots \\ E_i^{N-1} &= E_i^{N-1(0)} + E_i^{N-1(1)} + \cdots \\ E_a^{N+1} &= E_a^{N+1(0)} + E_a^{N+1(1)} + \cdots. \end{aligned} \tag{58}$$

By substituting into (2) and expanding, we can easily see that

$$\begin{aligned} G_{1qp}^{(1)}(\omega) = &\sum_a \frac{\left(b_{qa}^{(0)} b_{pa}^{(1)*} + b_{qa}^{(1)} b_{pa}^{(0)*}\right)}{\omega + E_0^{N(0)} - E_a^{N+1(0)} + i\varepsilon} \\ &+ \sum_i \frac{\left(b_{qi}^{(0)} b_{pi}^{(1)*} + b_{qi}^{(1)} b_{pi}^{(0)*}\right)}{\omega - E_0^{N(0)} + E_i^{N-1(0)} - i\varepsilon} \\ &+ \sum_a \frac{b_{qa}^{(0)} b_{pa}^{(0)*}(E_a^{N+1(1)} - E_0^{N(1)})}{(\omega + E_0^{N(0)} - E_a^{N+1(0)} + i\varepsilon)^2} \\ &+ \sum_i \frac{b_{qi}^{(0)} b_{pi}^{(0)*}(E_0^{N(1)} - E_i^{N-1(1)})}{(\omega - E_0^{N(0)} + E_i^{N-1(0)} - i\varepsilon)^2}. \end{aligned} \tag{59}$$

Evidently, the perturbed propagator has identical poles to the unperturbed form (1), except that there are poles of order 1 and order 2 (in terms of the Laurent expansion). Equation (59) can be reduced further by using a canonical transformation technique to expand the perturbed states $|\Psi_n^N\rangle$ in terms of the unperturbed ones. To this end, one introduces a unitary transformation

$$U = \exp(X) \tag{60}$$

in terms of an anti-Hermitian operator $X^\dagger = -X$. The perturbed states are now written in terms of the unperturbed ones as

$$|\Psi_n^N\rangle = U|\Psi_n^{N(0)}\rangle \tag{61}$$

and the Hamiltonian as

$$H = U(H^{(0)} + h^{(1)})U^\dagger. \tag{62}$$

To carry out the canonical transformations (61) and (62), we use the expansion

$$X = 1 + X^{(1)} + \cdots. \tag{63}$$

Assuming nondegenerate states for simplicity, the first-order perturbation equation is

$$\left\{[H^{(0)}, X^{(1)}]_- + h^{(1)} - E_n^{N(1)}\right\}|\Psi_n^{N(0)}\rangle = 0, \tag{64}$$

which leads to the formal solution

$$X^{(1)} = \sum_{N,\, n \neq m} |\Psi_m^{N(0)}\rangle \frac{\langle \Psi_m^{N(0)}|h^{(1)}|\Psi_n^{N(0)}\rangle}{E_n^{N(0)} - E_m^{N(0)}} \langle \Psi_n^{N(0)}|$$
$$E_n^{N(1)} = \langle \Psi_n^{N(0)}|h^{(1)}|\Psi_n^{N(0)}\rangle, \tag{65}$$

so that the perturbed Dyson orbital coefficients can be simplified as

$$\begin{aligned} b_{pi}^{(1)} &= \langle \Psi_0^{N(0)}|\left[a_p^+,\, X^{(1)}\right]_-|\Psi_i^{N-1(0)}\rangle \\ &= \sum_{j\neq i} \frac{\langle \Psi_0^{N(0)}|a_p^+|\Psi_j^{N-1(0)}\rangle\langle \Psi_j^{N-1(0)}|h^{(1)}|\Psi_i^{N-1(0)}\rangle}{E_i^{N-1(0)} - E_j^{N-1(0)}} \\ &\quad - \sum_{n\neq 0} \frac{\langle \Psi_0^{N(0)}|h^{(1)}|\Psi_n^{N(0)}\rangle\langle \Psi_n^{N(0)}|a_p^+|\Psi_i^{N-1(0)}\rangle}{E_n^{N(0)} - E_0^{N(0)}} \\ &= \sum_{j\neq i} \frac{b_{pj}^{(0)} h_{ji}^{(1)}}{E_i^{N-1(0)} - E_j^{N-1(0)}} + c_{pi}^{(1)}, \end{aligned} \tag{66}$$

where the contributions

$$c_{pi}^{(1)} = \sum_{n\neq 0} \frac{\langle \Psi_0^{N(0)}|h^{(1)}|\Psi_n^{N(0)}\rangle\langle \Psi_n^{N(0)}|a_p^+|\Psi_i^{N-1(0)}\rangle}{E_0^{N(0)} - E_n^{N(0)}} \tag{67}$$

are components of the perturbed Dyson orbital arising only from ground-state perturbations. Substituting (66) into (59) along with

$$\begin{aligned} E_0^{N(1)} - E_i^{N-1(1)} &= \langle \Psi_0^{N(0)}|h^{(1)}|\Psi_0^{N(0)}\rangle \\ &\quad - \langle \Psi_i^{N-1(0)}|h^{(1)}|\Psi_i^{N-1(0)}\rangle \end{aligned} \tag{68}$$

and similar equations for the attached states, one finds

$$\begin{aligned} G_{1qp}^{(1)}(\omega) &= \sum_a \frac{\left(c_{qa}^{(1)} b_{pa}^{(0)*} + b_{qa}^{(0)} c_{pa}^{(1)*}\right)}{\omega + E_0^{N(0)} - E_a^{N+1(0)} + i\varepsilon} \\ &\quad + \sum_i \frac{\left(c_{qi}^{(1)} b_{pi}^{(0)^*} - b_{qi}^{(0)} c_{pi}^{(1)*}\right)}{\omega + E_0^{N(0)} - E_i^{N-1(0)} - i\varepsilon} \\ &\quad + \sum_{a\neq b} \frac{b_{qa}^{(0)} h_{ab}^{(1)} b_{pb}^{(0)*}}{(E_b^{N+1(0)} - E_a^{N+1(0)})} \\ &\quad \times \left\{ \frac{1}{(\omega + E_0^{N(0)} - E_a^{N+1(0)} + i\varepsilon)} \right. \\ &\quad \left. - \frac{1}{(\omega + E_0^{N(0)} - E_b^{N+1(0)} + i\varepsilon)} \right\} \\ &\quad + \sum_{i\neq j} \frac{b_{qi}^{(0)} h_{ij}^{(1)} b_{pj}^{(0)*}}{\left(E_j^{N-1(0)} - E_i^{N-1(0)}\right)} \\ &\quad \times \left\{ \frac{1}{(\omega - E_0^{N(0)} + E_i^{N-1(0)} - i\varepsilon)} \right. \\ &\quad \left. - \frac{1}{\left(\omega - E_0^{N(0)} + E_j^{N-1(0)} - i\varepsilon\right)} \right\} \\ &\quad + \sum_a \frac{b_{qa}^{(0)}\left[h_{aa}^{(1)} - h_{00}^{(1)}\right] b_{pa}^{(0)*}}{(\omega + E_0^{N(0)} - E_a^{N+1(0)} + i\varepsilon)^2} \\ &\quad + \sum_i \frac{b_{qi}^{(0)}\left[h_{ii}^{(1)} - h_{00}^{(1)}\right] b_{pi}^{(0)*}}{(\omega - E_0^{N(0)} + E_i^{N-1(0)} - i\varepsilon)^2}. \end{aligned} \tag{69}$$

Introducing the fluctuation elements

$$\begin{aligned} \tilde{h}_{ab}^{(1)} &= \langle \Psi_a^{N+1(0)}|\left[h^{(1)} - \langle \Psi_0^{N(0)}|h^{(1)}|\Psi_0^{N(0)}\rangle\right]|\Psi_b^{N+1(0)}\rangle \\ \tilde{h}_{ij}^{(1)} &= \langle \Psi_i^{N-1(0)}|\left[h^{(1)} - \langle \Psi_0^{N(0)}|h^{(1)}|\Psi_0^{N(0)}\rangle\right]|\Psi_j^{N-1(0)}\rangle \end{aligned} \tag{70}$$

and factorizing the terms within the brackets, Eq. (69) can be further reduced as

$$\begin{aligned} G_{1qp}^{(1)}(\omega) &= \sum_a \frac{\left(c_{qa}^{(1)} b_{pa}^{(0)*} + b_{qa}^{(0)} c_{pa}^{(1)*}\right)}{\omega + E_0^{N(0)} - E_a^{N+1(0)} + i\varepsilon} \\ &\quad + \sum_a \frac{\left(c_{qi}^{(1)} b_{pi}^{(0)*} + b_{qi}^{(0)} c_{pi}^{(1)*}\right)}{\omega + E_0^{N(0)} - E_i^{N-1(0)} - i\varepsilon} \\ &\quad + \sum_{ab} \frac{b_{qa}^{(0)} \tilde{H}_{ab}^{(1)} b_{pb}^{(0)*}}{(\omega + E_0^{N(0)} - E_a^{N+1(0)} + i\varepsilon)\,(\omega + E_0^{N(0)} - E_b^{N+1(0)} + i\varepsilon)} \\ &\quad + \sum_{ij} \frac{b_{qi}^{(0)} \tilde{h}_{ij}^{(1)} b_{pj}^{(0)*}}{(\omega - E_0^{N(0)} + E_i^{N-1(0)} - i\varepsilon)\,\left(\omega - E_0^{N(0)} + E_j^{N-1(0)} - i\varepsilon\right)}. \end{aligned} \tag{71}$$

The structure of (70) is very familiar in perturbation theory. In diagrammatic terms, $\langle \Psi_0^{N(0)}|h^{(1)}|\Psi_0^{N(0)}\rangle$ refers to a fully contracted expansion of external field with respect to the ground-state wave function. This term acts to remove the unlinked clusters from the expansion of the fluctuation elements (71), ensuring therefore the size-consistency and size-extensivity of the CPEP approach at any order of its expansion [17]. It is obvious that the double pole terms in Eq. (71)

have zero residues in the Coulson integral and that the only contributions to the perturbed electron density come from the $c^{(1)}$ terms, viz.,

$$\begin{aligned}\rho^{(1)}_{1qp} &= \sum_i \left\{ c^{(1)}_{qi} b^{(0)*}_{pi} + b^{(0)}_{qi} c^{(1)*}_{pi} \right\} \\ &= \sum_i \langle \Psi_0^{N(0)} | a_p^+ | \Psi_i^{N-1(0)} \rangle \langle \Psi_i^{N-1(0)} | a_q X^{(1)} | \Psi_0^{N(0)} \rangle \\ &+ \sum_i \langle \Psi_0^{N(0)} | X^{(1)\dagger} a_p^+ | \Psi_i^{N-1(0)} \rangle \langle \Psi_i^{N-1(0)} | a_q | \Psi_0^{N(0)} \rangle \\ &= \langle \Psi_0^{N(0)} | \left[a_p^+ a_q, X^{(1)} \right]_- | \Psi_0^{N(0)} \rangle, \end{aligned} \tag{72}$$

which is the correct result. An important outcome of this equation is the anti-Hermitian character of $\boldsymbol{\rho}^{(1)}$. From (67) and (72), it appears also that the exact perturbed electron density only relates to the Dyson orbital coefficients arising from the ionization sector of the unperturbed propagator.

The Perturbed Self-energy

So far, we have explored the formal structure of the perturbed Green's function. In practice, we need an approximate treatment. The starting point for this is the explicit superoperator representation (18), together with (23) and the expression for the self-energy (41). The treatment is carried out explicitly by expanding each block implied in (18) such as

$$\begin{aligned} \mathbf{H}^{aa} &= \mathbf{H}^{aa(0)} + \mathbf{H}^{aa(1)} + \cdots \\ \mathbf{H}^{ab} &= \mathbf{H}^{ab(0)} + \mathbf{H}^{ab(1)} + \cdots . \\ &\vdots \end{aligned} \tag{73}$$

Through the first order in the external field, one finds

$$\begin{aligned} \mathbf{G}_1^{-1}(\omega) = \omega \mathbf{1}^{aa} &- \mathbf{H}^{aa(0)} \\ &- \left(\mathbf{H}^{ab(0)} (\omega \mathbf{S}^{bb(0)} - \mathbf{H}^{bb(0)})^{-1} \mathbf{H}^{ba(0)} \right) \\ &- \mathbf{H}^{aa(1)} - \mathbf{H}^{ab(1)} (\omega \mathbf{S}^{bb(0)} - \mathbf{H}^{bb(0)})^{-1} \\ &\times \mathbf{H}^{ba(0)} - \mathbf{H}^{ab(0)} (\omega \mathbf{S}^{bb(0)} - \mathbf{H}^{bb(0)})^{-1} \\ &\times \mathbf{H}^{ba(1)} - \mathbf{Q}^{(1)}(\omega), \end{aligned} \tag{74}$$

where the quadratic part $\mathbf{Q}^{(1)}(\omega)$ is defined as

$$\begin{aligned} \mathbf{Q}^{(1)} = \mathbf{H}^{ab(0)} (\omega \mathbf{S}^{bb(0)} - \mathbf{H}^{bb(0)})^{-1} (\mathbf{H}^{bb(1)} - \omega \mathbf{S}^{bb(1)}) \\ \times (\omega \mathbf{S}^{bb(0)} - \mathbf{H}^{bb(0)})^{-1} \mathbf{H}^{ba(0)}. \end{aligned} \tag{75}$$

Alternatively, from Eqs. (50) and (54), one can also consistently expand the perturbed propagator through first order as

$$\begin{aligned} \mathbf{G}_1^{-1}(\omega) = \omega \mathbf{1}^{aa} &- (\mathbf{F}^{(0)} + \mathbf{M}^{(0)}(\omega)) \\ &- (\mathbf{F}^{(1)} + \mathbf{M}^{(1)}(\omega)). \end{aligned} \tag{76}$$

Expanding, as previously [Eq. (60)–(65)], the exact wave function from the unperturbed ground state by means of a unitary transformation, it is easy to show that

$$\begin{aligned} H^{aa(1)}_{pq} &= \langle \Psi_0^{N(0)} | \left[a_p^+, \left[h^{(1)}, a_q \right]_- \right]_+ | \Psi_0^{N(0)} \rangle \\ &+ \langle \Psi_0^{N(0)} | \left[\left[a_p^+, \left[H^{(0)}, a_q \right]_- \right]_+, X^{(1)} \right]_- | \Psi_0^{N(0)} \rangle \\ &= h^{(1)}_{pq} + \sum_{rs} \langle pr || qs \rangle \rho^{(1)}_{1sr} = F^{(1)}_{pq}, \end{aligned} \tag{77}$$

which accounts for the constant part of the first-order perturbed self-energy. Therefore, comparing Eqs. (74) and (76) together with Eqs. (25), (45), and (77), it follows that

$$\begin{aligned} \mathbf{M}^{(1)}(\omega) = \mathbf{H}^{ab(1)} (\omega \mathbf{S}^{bb(0)} - \mathbf{H}^{bb(0)})^{-1} \mathbf{H}^{ba(0)} \\ + \mathbf{H}^{ab(0)} (\omega \mathbf{S}^{bb(0)} - \mathbf{H}^{bb(0)})^{-1} \mathbf{H}^{ba(1)} \\ + Q^{(1)}(\omega). \end{aligned} \tag{78}$$

Equation (78) represents an exact form of the first-order perturbed dynamic self-energy. It is now necessary to produce explicit expressions for the perturbed self-energy by expanding it order by order in terms of the correlation potential. At this point, it is interesting to note that, as in the unperturbed case, the perturbed dynamic self-energy presents a pole structure similar to the one of the perturbed one-electron propagator (59).

As for the unperturbed self-energy (45), several approximations to $\boldsymbol{\Sigma}^{(1)}$ can be constructed depending on the extension of the complementary orthogonalized manifold of operators, b, and the nature of the wave function used to expand the binary products. As for the unperturbed propagator, the simplest approximation to Eq. (78) is derived by restricting b to the first complementary set (21) and taking the HF wave function as the reference ground state.

To derive through first order in the external field and in correlation the perturbed overlap $\mathbf{S}^{bb}$ matrix, one must expand to those orders the one-body and two-body densities. From expression (72), one finds readily the well-known coupled

Hartree–Fock (CPHF) equations [24, 25] for $\boldsymbol{\rho}_1^{(1)}$:

$$\begin{aligned}\rho_{1qp}^{(1)[1]} &= \sum_{rs} \langle \Psi_0^{N(0)[1]} | [\, a_p^+ a_q \,,\, a_r^+ a_s \,]_- | \Psi_0^{N(0)[1]} \rangle X_{rs}^{(1)[1]} \\ &= \sum_s X_{qs}^{(1)} \rho_{1sp}^{(0)[1]} - \sum_r X_{rp}^{(1)} \rho_{1qr}^{(0)[1]} \\ &= X_{qp}^{(1)} \big(\bar{n}_q n_p - \bar{n}_p n_q \big), \end{aligned} \tag{79}$$

where the coupling between particle and hole states is given by

$$X_{qp}^{(1)} = \frac{F_{qp}^{(1)}\big(\rho_{qp}^{(1)[1]} \big)}{\epsilon_p - \epsilon_q} \big(\bar{n}_q n_p + \bar{n}_p n_q \big). \tag{80}$$

Similarly, for the perturbed two-body density, one finds, at the HF level,

$$\begin{aligned}\rho_{2rs,\,pq}^{(1)[1]} &= \sum_{tu} \langle \Psi_0^{N(0)[1]} | [\, a_p^+ a_q^+ a_s a_r \,,\, a_t^+ a_u \,]_- \\ &\quad | \Psi_0^{N(0)[1]} \rangle X_{tu}^{(1)} \\ &= (1 - P_{pq})(1 - P_{rs})\, X_{rp}^{(1)} \delta_{qs} \\ &\quad \times \big(n_p n_q \bar{n}_r n_s - \bar{n}_p n_q n_r n_s \big). \end{aligned} \tag{81}$$

After considerable effort, it can than be shown that Eq. (26) yields, to first order in the external field, the following expression:

$$\begin{aligned} S_{q'r's',\,qrs}^{bb(1)[1]} &= (1 - P_{rs})(1 - P_{r's'}) \\ &\quad \times \left\{ \begin{array}{l} \delta_{qq'} \delta_{rr'} X_{ss'}^{(1)} (n_s - \bar{n}_s) \big(n_q \bar{n}_r - \bar{n}_q n_r \big) \\ + \delta_{rr'} \delta_{ss'} X_{qq'}^{(1)} \bar{n}_s (n_q - \bar{n}_q) \end{array} \right\}. \end{aligned} \tag{82}$$

When restricting the h_3 operator manifold to the 2h–1p and 2p–1h configuration subspaces, Eq. (82) simply reverts to

$$\mathbf{S}^{bb(1)[1]} = \mathbf{0}^{bb}. \tag{83}$$

This hinges on the fact that no part of Eq. (82) couples the *aij* to the *a′i′j′* indices (and, similarly, in the 2p–1h sector). From this together with Eq. (40), the first-order perturbed self-energy therefore becomes

$$\begin{aligned} \mathbf{M}^{(1)}(\omega) &= \mathbf{H}^{ab(1)} (\omega \mathbf{1}^{bb} - \mathbf{H}^{bb(0)})^{-1} \mathbf{H}^{ba(0)} \\ &\quad + \mathbf{H}^{ab(0)} (\omega \mathbf{1}^{bb} - \mathbf{H}^{bb(0)})^{-1} \mathbf{H}^{ba(1)} \\ &\quad + \mathbf{Q}^{(1)}(\omega), \end{aligned} \tag{84}$$

where the quadratic part now takes the form

$$\begin{aligned} \mathbf{Q}^{(1)}(\omega) &= \mathbf{H}^{ab(0)} (\omega \mathbf{1}^{bb} - \mathbf{H}^{bb(0)})^{-1} \mathbf{H}^{bb(1)} \\ &\quad \times (\omega \mathbf{1}^{bb} - \mathbf{H}^{bb(0)})^{-1} \mathbf{H}^{ba(0)}. \end{aligned} \tag{85}$$

As the binary products $\mathbf{H}^{ab(0)}$ and $\mathbf{H}^{ba(0)}$ based on the HF reference ground state are of first order in correlation [see Eq. (41)], and as the related $\mathbf{H}^{bb(0)[1]}$ matrix given in (42) contains zeroth-order and first-order terms, the perturbed coupling amplitudes $\mathbf{H}^{ab(1)}$ and $\mathbf{H}^{ba(1)}$ have also to be expanded up to first order to ensure a second-order expansion of Eq. (84). On the other hand, a zeroth-order form of $\mathbf{H}^{bb(1)}$ is sufficient for a second-order expansion of the quadratic term (85).

To ensure an expansion of $\mathbf{M}^{(1)}(\omega)$ which is correct up to third order in correlation, one has to include appropriate correlation corrections to the ground-state densities used to expand the binary products. There is no need to expand the operator manifold to the h_5 subset, since this relates to geometric series of fourth- and higher-order terms. There is also no need to bypass the first-order (i.e., HF) level for the $\mathbf{S}^{bb(0)}$, $\mathbf{H}^{bb(0)}$, $\mathbf{S}^{bb(1)}$, and $\mathbf{H}^{bb(1)}$ blocks, since, as for the unperturbed self-energy, correlation corrections to these matrices would yield terms that are at least of fourth order in correlation [this implies that Eq. (85) holds also at third order]. On the other hand, both perturbed and unperturbed off-diagonal blocks $\mathbf{H}^{ab(0)}$, $\mathbf{H}^{ab(1)}$, $\mathbf{H}^{ba(0)}$, and $\mathbf{H}^{ba(1)}$ will have to be expanded consistently to second order.

As with the unperturbed self-energy, correlation corrections to the ground-state perturbed density must also result into a constant contribution to the perturbed self-energy. Constant contributions may also arise from a polarization of the bielectron interactions, which probe the external field according to the following perturbation series:

$$|s'\rangle = |s\rangle + \sum_t \frac{F_{ts}^{(1)}}{\epsilon_s - \epsilon_t} |t\rangle \cdots \tag{86}$$

for the one-electron states. Considering Eq. (46) as the starting point for an expansion of $\boldsymbol{\Sigma}(\infty)$ in terms of the external field, the constant part of the first-order perturbed self-energy can then be obtained as

$$\begin{aligned} \Sigma_{pq}^{(1)}(\infty) &= \sum_{rs} \langle\, pr \,||\, qs \,\rangle \rho_{1sr}^{(1)[corr]} \\ &\quad + \sum_{rt} \langle\, pr \,||\, qt \,\rangle \\ &\quad \times \sum_s \{ \alpha_{ts}^{(1)} \rho_{1sr}^{(0)[corr]} - \rho_{1ts}^{(0)[corr]} \sigma_{sr}^{(1)*} \}, \end{aligned} \tag{87}$$

where the anti-Hermitian matrix $\boldsymbol{\alpha}$ accounts for the one-electron transition density

$$\alpha_{ts}^{(1)} = (1 - \delta_{ts}) \frac{F_{ts}^{(1)}}{\epsilon_s - \epsilon_t} = -\alpha_{st}^{(1)*} \qquad (88)$$

When only real one-electron states are considered, the terms in brackets identically cancel, as a result of the antisymmetry properties of one-electron transition densities and products of such matrices with ground-state one-electron densities. The constant part of the perturbed density therefore only arises from the correlation part of the perturbed density:

$$\Sigma_{pq}^{(1)}(\infty) = \sum_{rs} \langle pr||qs\rangle \rho_{1sr}^{(1)[corr]} \qquad (89)$$

The 2ph-TDA Perturbed Self-energy

In the preceding section, we have gained information about the analytic and basic matrix structures of the perturbed self-energy. We now exploit this information to derive a systematic scheme to expand $\boldsymbol{\Sigma}^{(1)}$ beyond second order in correlation. From now on, we will extensively make use of the diagrammatic approach to a double perturbation theory [47], which, by its simplicity and straightforward nature, helps in preselecting the more important contributions and gives a direct physical insight.

The diagrammatic rules used in this work have been fully described in a former contribution [41]. As previously [17, 41], our basic diagrammatic ingredients will be the dot-vertex [Fig. 1(a)] used to represent antisymmetrized bielectron integrals according to the conventions of Hugenholtz or Abrikosov [48–51] and the cross vertex of Figure 1(b) standing for the $F_{pq}^{(1)}$ matrix elements, defined as transition elements over the first-order perturbed Fock operator. At this point, it is useful to remember that the self-dependence of the perturbed electron density through $\mathbf{G}_1^{(1)}$ and $\mathbf{F}^{(1)}$ implies already a renormalization of the transition elements over the external field. The more obvious example is given by the CPHF Eqs. (79) and (80) for $\boldsymbol{\rho}_1^{(1)}$, in which the self-dependence of the perturbed density results [41] in diagrammatic terms in a screening of the external field through the interplay of an infinite geometric series of diagrams of RPA [52] (i.e., ''ring'' or ''bubble'') character.

The starting point of a 2ph-TDA [or ADC (2)] derivation of the perturbed self-energy is Eqs. (84) and (85), sketched diagrammatically (Fig. 2) in terms of dot-vertices, contraction lines, and some additional symbols, such as the 2p−1h or 2h−1p kernels, a polarized dot-vertex, and an hexagonal cluster. Each of these kernel and vertices account for one of the matrix blocks implies in Eqs. (84), and (85), i.e., $(\omega \mathbf{1}^{bb} - \mathbf{H}^{bb(0)[1]})^{-1}$, $\mathbf{H}^{ab(1)}$ or $\mathbf{H}^{ba(1)}$, and $\mathbf{H}^{bb(1)}$, respectively. The dot-vertices in Figure

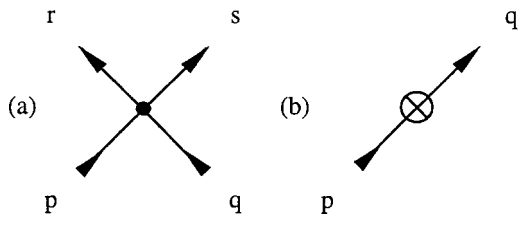

FIGURE 1. The elementary (a) dot and (b) cross vertices, standing for anti-symmetrized two-electron integrals and matrix elements over the first-order perturbed Fock operator, respectively.

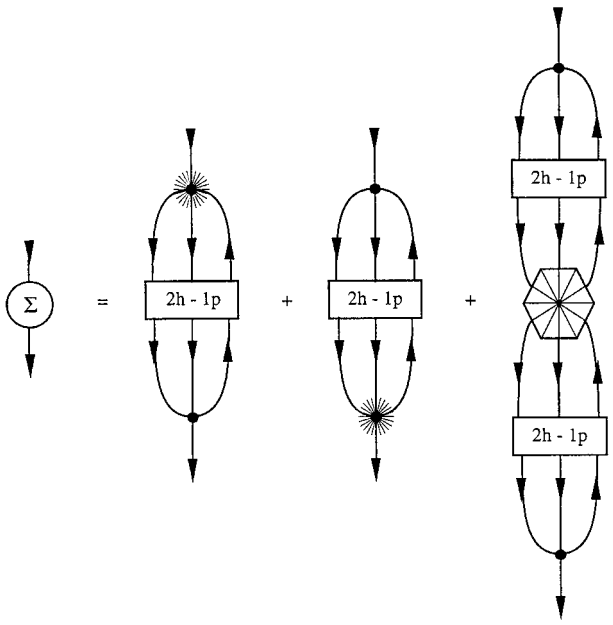

FIGURE 2. Schematic ADC(2) expansion of the advanced (hole) part of $\boldsymbol{\Sigma}(\omega)$ in terms of first-order polarized dot-vertices (indicated by a star) of the 2h−1p (two holes, one particle) kernel, and of the $\mathbf{H}^{bb(1)}$ coupling amplitude (displayed as an hexagonal cluster).

2 can be readily related to the $\mathbf{H}^{ab(0)[1]}$ and $\mathbf{H}^{ba(0)[1]}$ coupling amplitudes as given in (41). As we make explicit, in more detail a few lines below, the matrix $(\omega\mathbf{1}^{bb} - \mathbf{H}^{bb(0)[1]})^{-1}$ is well known and accounts, by virtue of the inverse, for an infinite partial summation over well-defined types of diagrams. The nature of the other vertices is at this stage still undefined. The polarized dot-vertex and the hexagon cluster relate to some diagrammatic substructures, which by construction have to fit with the 12 time-ordered (Goldstone) diagrams accounting [41] for the second-order perturbed self-energy. To understand fully the principles of our direct diagrammatic construction scheme for $\mathbf{H}^{ab(1)[1]}$ or $\mathbf{H}^{ba(1)[1]}$, and $\mathbf{H}^{bb(1)[0]}$, one should note that these terms simply account for a polarization through first order in the external field of the bielectron interactions and the three-body kernels. All the second-order perturbed self-energy diagrams with the cross-vertex falling *inside* the kernel therefore yield contributions to $\mathbf{H}^{bb(1)[0]}$, while the off-diagonal $\mathbf{H}^{ab(0)[1]}$ and $\mathbf{H}^{ba(0)[1]}$ terms relate to second-order diagrams with the cross vertex falling *outside* the kernel. On these considerations, one can then easily bypass the comparison procedure required for an ADC(2) expansion.

As in the work by Schirmer and Cederbaum [33], the 2h−1p and 2p−1h kernels correspond to the linear two-hole-one-particle and two-particle-one-hole linear responses related to the advanced (hole) and retarded (particle) sectors of the unperturbed self-energy, respectively. These kernels are consistently expanded up to first-order with regard to the correlation potential, using the iterative equation displayed in Figure 3. From this expansion, at the root of a 2ph−TDA renormalization, it follows that an infinite geometric series of contributions of mixed ''ladder''/''ring'' character is implied in the expansion of $\mathbf{M}^{(1)}$. This can be alternatively assessed from a Born expansion [53] of the corresponding matrix inverse $(\omega\mathbf{1}^{bb} - \mathbf{H}^{bb(0)[1]})^{-1}$, using (42) to evaluate the effective energy interaction $\mathbf{H}^{bb(0)[1]}$. The factor $\frac{1}{2}$ in Eqs. (42) finds its origin in the symmetry interchange properties of unrestricted indices i and j, or a and b, respectively. Diagrammatically speaking, it is needed to avoid the overcounting of ladder-type diagrams, exhibiting multiple topological degeneracies in the form of equivalent contraction lines.

The 2ph-TDA corrections to the unperturbed 2p−1h and 2h−1p excitation energies account for a major part of the collective effects that arise within the $N \pm 1$ electron systems. In many cases, their influence on the computed ionization or electroattachment energies have been shown to be equivalent if not bigger than the changes arising from second-order corrections to the HF values, yielding a much better agreement with experiment. Since the 2ph − TDA renormalization usually affects drastically the pole strengths and, hence, Dyson orbital coefficients, it might then also significantly improve the quality of the perturbed electron density and of CPEP linear responses.

The polarized dot-vertices standing for $\mathbf{H}^{ab(1)}$ and $\mathbf{H}^{ba(1)}$ are diagrammatically expanded in Figure 4. This in done in terms of all the graphs which yield the second-order perturbed self-energy diagrams characterized by the external location of the cross-vertex with respect to the kernel (i.e., the $\mathbf{C}_1$, $\mathbf{C}_2$, $\mathbf{D}_1$, $\mathbf{D}_2$, $\mathbf{G}_1$, $\mathbf{G}_2$, $\mathbf{H}_1$, and $\mathbf{H}_2$ graphs displayed in [41]) when they are inserted in Figure 2. At first order with respect to correlation, the graphs of Figure 4 correspond strictly to bielectron integrals polarized [23] up to first order under the external field. Applying the diagrammatic rules in the usual way, these graphs can be readily translated into

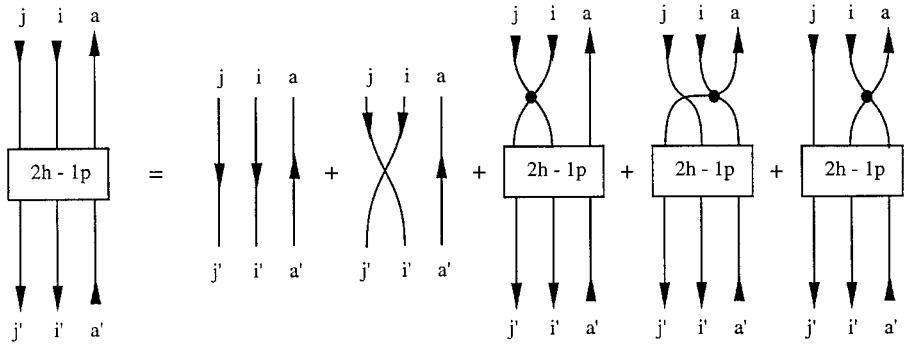

FIGURE 3. The 2ph-TDA renormalization of the 2h −1p kernel (adapted from [33]).

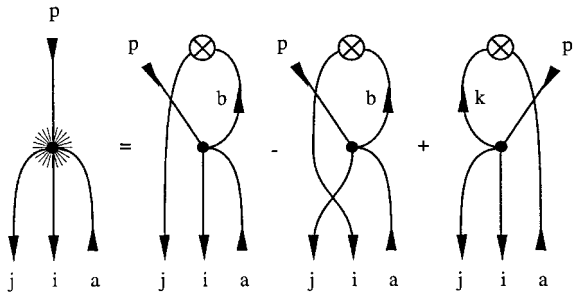

FIGURE 4. The perturbed $H^{13}_{p,aij}(1)[1]$ coupling amplitude, displayed as a polarized dot-vertex.

algebraic form:

$$
\begin{aligned}
H^{13(1)[1]}_{p,aij} &= (1 - P_{ij}) \sum_b \frac{F^{(1)}_{bj} \langle pa||bi\rangle}{(\varepsilon_j - \varepsilon_b)} \\
&\quad - \sum_k \frac{F^{(1)}_{ak} \langle pk||ik\rangle}{(\varepsilon_k - \varepsilon_a)} \\
H^{13(1)[1]}_{p,iab} &= -(1 - P_{ab}) \sum_k \frac{F^{(1)}_{kb} \langle pi||ka\rangle}{(\varepsilon_k - \varepsilon_b)} \\
&\quad + \sum_c \frac{F^{(1)}_{ic} \langle pc||ab\rangle}{(\varepsilon_i - \varepsilon_c)} \\
H^{31(1)[1]}_{aij,q} &= (1 - P_{ij}) \sum_b \frac{F^{(1)}_{jb} \langle bi||qa\rangle}{(\varepsilon_j - \varepsilon_b)} \\
&\quad - \sum_k \frac{F^{(1)}_{ka} \langle ij||qk\rangle}{(\varepsilon_k - \varepsilon_a)} \\
H^{31(1)[1]}_{iab,q} &= -(1 - P_{ab}) \sum_k \frac{F^{(1)}_{bk} \langle ka||qi\rangle}{(\varepsilon_k - \varepsilon_b)} \\
&\quad + \sum_c \frac{F^{(1)}_{ci} \langle ab||qc\rangle}{(\varepsilon_i - \varepsilon_c)}. \qquad (90)
\end{aligned}
$$

By inserting these expressions into Eq. (84), one can easily check that they fit with the second-order $\mathbf{C}_1$, $\mathbf{C}_2$, $\mathbf{D}_1$, $\mathbf{D}_2$, $\mathbf{G}_1$, $\mathbf{G}_2$, $\mathbf{H}_1$, and $\mathbf{H}_2$ perturbed self-energy contributions derived in previous works [23, 41]).

An essential and particular ingredient in the expansion of the 2ph-TDA perturbed self-energy is the hexagon introduced in Figure 2 to represent the six-entry perturbed coupling amplitudes, $\mathbf{H}^{bb(1)}$, defined with respect to the 2h−1p shape-up and 2p−1h shake-on configuration spaces generated by the h_3 operator manifold. From Eq. (85), it follows that no frequency dependence arises from that symbol, which one can therefore regard as a cluster dividing the kernel of the quadratic part of the perturbed self-energy into two frequency-dependent subkernels. By construction, the hexagonal cluster must describe the influence of the external field on the 2p−1h and 2h−1p excitation energies, either in their zeroth-order form with regard to correlation or renormalized through the interplay of a 2ph-TDA expansion. Once inserted in Figure 2, this vertex must therefore yield the second-order **A**, **B**, **E**, and **F** perturbed self-energy diagrams displayed in [41], in which the cross-vertex falls inside the kernel. Like the dot-vertex and polarized dot-vertex, the hexagon-cluster must also preserve the antisymmetry interchange properties of the indices associated with equivalent contraction lines, i.e., in this case, indices (i, j) and (i', j') for $H^{bb(1)}_{ija,i'j'a'}$ or indices (a, b) and (a', b') for $H^{bb(1)}_{abi,a'b'i'}$. From now on, the requested interchange properties of equivalent contraction lines will be ensured using the antisymmetrizers displayed in Figure 5, to be translated as

$$
\begin{aligned}
A_{ij,i'j'} &= \delta_{ii'}\delta_{jj'} - \delta_{ij'}\delta_{i'j} = (1 - P_{ij})\delta_{ii'}\delta_{jj'} \\
&= (1 - P_{i'j'})\delta_{ii'}\delta_{jj'} \\
A_{ab,a'b'} &= \delta_{aa'}\delta_{bb'} - \delta_{ab'}\delta_{a'b} = (1 - P_{ab})\delta_{aa'}\delta_{bb'} \\
&= (1 - P_{a'b'})\delta_{aa'}\delta_{bb'}. \qquad (91)
\end{aligned}
$$

To evaluate algebraically the zeroth-order form of the hexagon-cluster in a 2ph-TDA expansion, one can first proceed by a direct comparison with

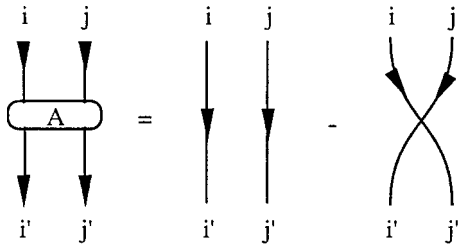

FIGURE 5. The antisymmetrizer $A_{ij,i'j'}$.

the second-order **A**, **B**, **E**, and **F** perturbed self-energy contributions derived in [41]. More precisely, one has to restrict the 2p−1h and 2h−1p linear responses to their zeroth-order form and extract all the second-order contributions to be found from the generic expressions:

$$M_{pq}^{h(1)[2]} = -\frac{1}{4}\sum_{ija}\sum_{i'j'a'}\frac{\langle pa||ij\rangle H^{bb(1)}_{ija,i'j'a'}\langle i'j'||qa'\rangle}{(\omega+\varepsilon_a-\varepsilon_i-\varepsilon_j)(\omega+\varepsilon_{a'}-\varepsilon_{i'}-\varepsilon_{j'})}$$

$$M_{pq}^{p(1)[2]} = +\frac{1}{4}\sum_{iab}\sum_{i'a'b'}\frac{\langle pi||ab\rangle H^{bb(1)}_{abi,a'b'i'}\langle a'b'||qi'\rangle}{(\omega+\varepsilon_i-\varepsilon_a-\varepsilon_b)(\omega+\varepsilon_{i'}-\varepsilon_{a'}-\varepsilon_{b'})} \quad (92)$$

in which topological degeneracies arising from the presence of equivalent contraction lines and the number of hole lines and closed fermion loops have been considered. Alternatively, one can directly evaluate the diagrams displayed in Figure 6 as

$$H^{33(1)[0]}_{ija,i'j'a'} = (1-P_{ij})(1-P_{i'j'})\times\left\{-\delta_{aa'}\delta_{ii'}F^{(1)}_{jj'}+\delta_{ii'}\delta_{jj'}F^{(1)}_{aa'}\right\}$$

$$H^{33(1)[]0}_{abi,a'b'i'} = (1-P_{ab})(1-P_{a'b'})\times\{\delta_{ii'}\delta_{aa'}F^{(1)}_{bb'}-\delta_{aa'}\delta_{bb'}F^{(1)}_{ii'}\}. \quad (93)$$

By inserting this result into Eqs. (92) and comparing with former derivations [41], one can easily assess the consistency of our direct diagrammatic construction scheme.

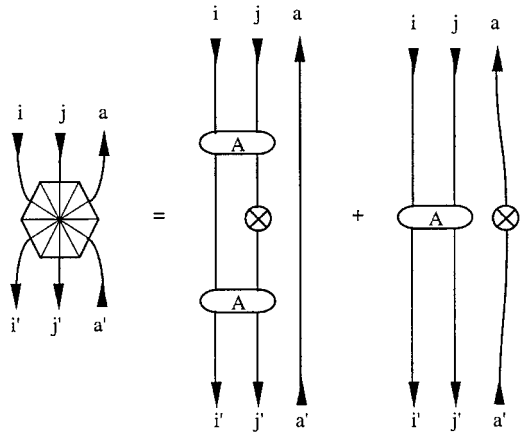

FIGURE 6. Diagrammatic expansion of the $H^{33(1)[0]}_{ija,i'j'a}$ coupling amplitude.

The Extended 2ph-TDA Perturbed Self-energy

Our direct derivation of the 2ph-TDA/ADC(2) scheme has recovered the rather simple second-order approximation scheme for $\mathbf{\Sigma}^{(1)}(\omega)$. The particular benefit of this approach will now become apparent from the construction of the extended 2ph-TDA/ADC(3) scheme. This, certainly, represents a considerable task: in third order with respect to correlation, one has to deal (Fig. 7) with four Feynman diagrams for $\mathbf{\Sigma}^{(1)}(\infty)$ and eight Feynman diagrams for $\mathbf{M}^{(1)}(\omega)$, each generating 24 time orderings (in terms of Goldstone diagrams), yielding a total of 96 constant and 192 dynamic perturbed self-energy contributions. As a main example, we display in Figure 8 the 12 time-orderings corresponding to the hole sector of one of the perturbed ladder-type diagrams given in Figure 7. In spite of this at-first-glance intimidating situa-

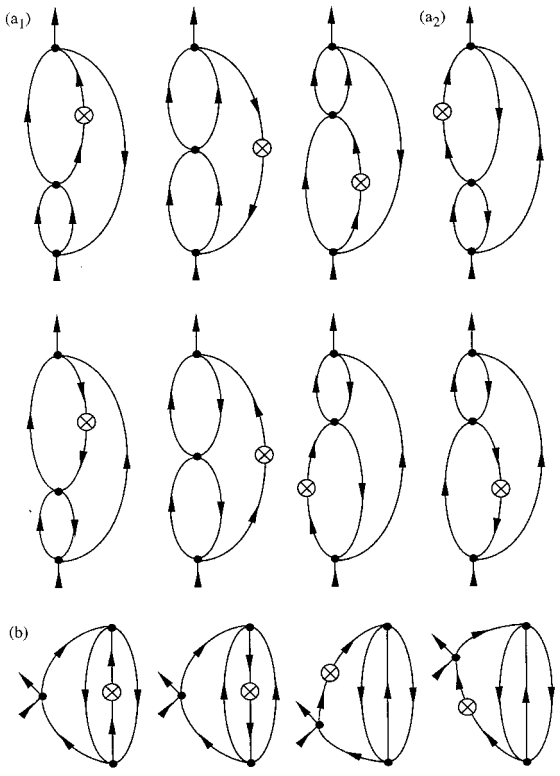

FIGURE 7. The 12 Feynman diagrams accounting for (a) $\mathbf{M}^{(1)}(\omega)$ and (b) $\mathbf{\Sigma}^{(1)}(\infty)$. Set (a) can furthermore be divided in terms of diagrams of (a1) ''ladder' and (a2) ''ring'' character.

tion, one can efficiently and in a straightforward manner carry out this expansion, since these diagrams relate only to multiple combinations of a rather limited number of subgraphs, which, as the polarized dot-vertex of the previous section, can themselves be easily expanded from simpler diagrammatic structures.

The zeroth-order hexagon-cluster, the polarized dot-vertex, and the three-body kernels introduced in the previous section are the very first elements of our construction game for $\mathbf{\Sigma}^{(1)}(\omega)$. By inserting these subgraphs in Figure 2, one can already construct 40 of the 192 diagrams accounting for $\mathbf{M}^{(1)[3]}$, such as the **A** and **B** graphs of Figure 8, obtained as a combination of the 2h−1p kernel with $\mathbf{H}^{bb(1)[0]}$ or with $\mathbf{H}^{ab(1)[1]}$, respectively.

To proceed through third order, however, our diagrammatic kit must be extended by some additional elements, incorporating the required correlation corrections to the ground-state density. As can be intuitively understood, electronic correlation in the ground-state many-body wave function accounts for a screening of the Coulomb interactions between bare particles. In the context of Green's function theory, ground-state electronic correlation attenuates the internal dynamic polarization effects induced by the propagation of an additional charged particle (electron or hole), as it as been numerically observed in many situations (for instance, see [14, 16]). Similarly, it tends also to decrease the induced (bielectron) part of the response of a many-electron system to an external field. It is therefore natural to mimick diagrammatically Eqs. (84) and (85) by means of the graphs displayed in Figure 9, in which the bar dot-vertices and polarized dot-vertices of Figure 2 appear now as screened interaction elements. At this point, it is useful to recall that a consistent third-order derivation of $\mathbf{M}^{(1)}(\omega)$ implies a first-order expansion of the $\mathbf{H}^{bb(1)}$ block (alias the hexagon-cluster), while second-order correlation corrections have to be considered for the $\mathbf{H}^{ab(0)}$ and $\mathbf{H}^{ba(0)}$ blocks or the $\mathbf{H}^{ab(1)}$ and $\mathbf{H}^{ba(1)}$ blocks (alias the screened dot-vertices and screened polarized dot-vertices, respectively). As with ADC(2), incomplete series ex-

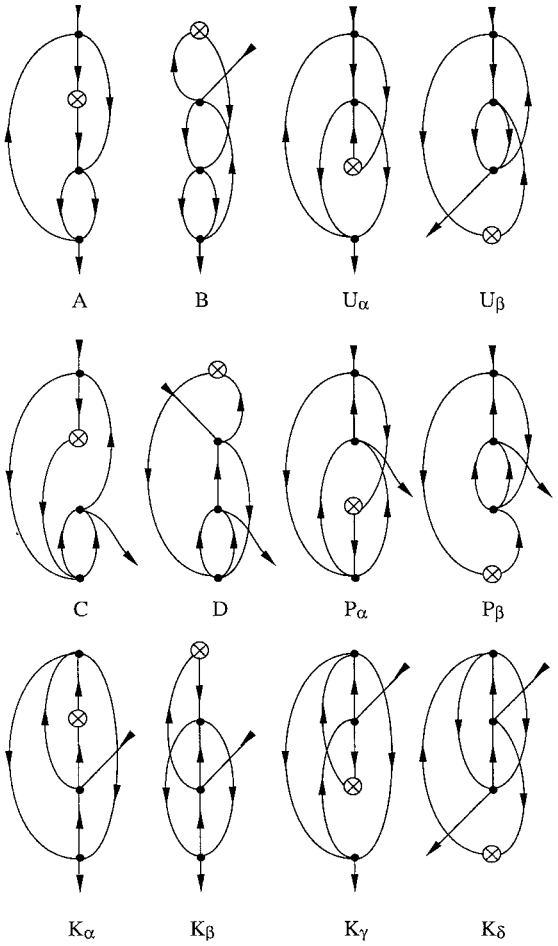

FIGURE 8. The 12 time-orderings corresponding to the first diagram of Figure 7, in the hole sector of $\mathbf{M}^{(1)}(\omega)$.

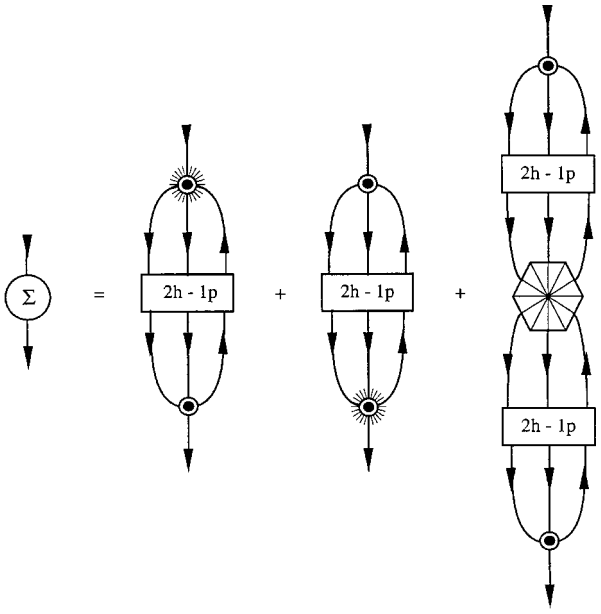

FIGURE 9. ADC(3) extension of Figure 2 to the correlation effects in the ground state, implying a screening of all coupling amplitudes.

tending beyond third order will be included through the 2ph-TDA renormalization of the 2p−1h and 2h−1p kernels.

In analogy with the effect of the field on the $\mathbf{H}^{ab(1)[1]}$ and $\mathbf{H}^{ba(1)[1]}$ interactions, electronic correlation in the ground state yields dynamic third-order unperturbed self-energy diagrams (the $\mathbf{C}_2$ to $\mathbf{C}_5$ to $\mathbf{D}_2$ to $\mathbf{D}_5$ graphs given in [3]) differing from the second-order terms by the presence of an additional dot-vertex falling *outside* the 2p−1h or 2h−1p kernels. These diagrams can also be obtained [14] by inserting the screened dot-vertices of Figure 10 in the second-order unperturbed self-energy graphs. Similar diagrammatic substructures take part, together with the zeroth-order hexagon-cluster or the polarized dot-vertex, in the construction of 40 more perturbed third-order self-energy diagrams, such as the **C** and **D** graphs given in Figure 8. Applying diagrammatic rules in the usual manner, the corresponding matrices can then readily be evaluated as

$$H^{13(0)[2]}_{p,aij} = \langle pa||ij\rangle + \frac{1}{2}\sum_{bc}\frac{\langle pa||bc\rangle\langle bc||ij\rangle}{\varepsilon_i+\varepsilon_j-\varepsilon_b-\varepsilon_c} - (1-P_{ij})\sum_{bk}\frac{\langle pk||bi\rangle\langle ab||jk\rangle}{\varepsilon_j+\varepsilon_k-\varepsilon_a-\varepsilon_b}$$

$$H^{13(0)[2]}_{p,iab} = \langle pi||ab\rangle + \frac{1}{2}\sum_{jk}\frac{\langle pi||jk\rangle\langle jk||ab\rangle}{\varepsilon_j+\varepsilon_k-\varepsilon_a-\varepsilon_b} - (1-P_{ab})\sum_{cj}\frac{\langle pc||ja\rangle\langle ij||bc\rangle}{\varepsilon_i+\varepsilon_j-\varepsilon_b-\varepsilon_c}$$

$$H^{31(0)[2]}_{aij,q} = \langle ij||qa\rangle + \frac{1}{2}\sum_{bc}\frac{\langle ij||bc\rangle\langle bc||qa\rangle}{\varepsilon_i+\varepsilon_j-\varepsilon_b-\varepsilon_c} - (1-P_{ij})\sum_{bk}\frac{\langle jk||ab\rangle\langle bi||qk\rangle}{\varepsilon_j+\varepsilon_k-\varepsilon_a-\varepsilon_b}$$

$$H^{31(0)[2]}_{iab,q} = \langle ab||qi\rangle + \frac{1}{2}\sum_{jk}\frac{\langle ab||jk\rangle\langle jk||qi\rangle}{\varepsilon_j+\varepsilon_k-\varepsilon_a-\varepsilon_b} - (1-P_{ab})\sum_{cj}\frac{\langle ij||bc\rangle\langle ja||qc\rangle}{\varepsilon_i+\varepsilon_j-\varepsilon_b-\varepsilon_c}, \quad (94)$$

which are precisely the equations obtained for these blocks by Baker [32] or Schirmer et al. [34, 35].

Similarly, the second-order correlation corrections in the $\mathbf{H}^{ab(1)[2]}$ and $\mathbf{H}^{ba(1)[2]}$ blocks have also clearly to yield all the remaining third-order perturbed time-ordered self-energy diagrams characterized by the *external* location, with respect to the kernel, of one of the dot-vertices, such as the **P** and **K** graphs displayed in Figure 8. All diagrams in the **P** and **K** series relate to the same skeleton structure and differ only by the time location of the cross-vertex. The corresponding algebraic expressions are

$$P_{\alpha_{pq}}(\omega) = \frac{1}{2}\sum_{abc}\sum_{ijk}\frac{\langle pa||ij\rangle F^{(1)}_{iln}\langle jk||bc\rangle\langle bc||qa\rangle}{D^{\omega a}_{ij}D^{bc}_{ij}D^{bc}_{jk}}$$

$$P_{\beta_{pq}}(\omega) = -\frac{1}{2}\sum_{abcd}\sum_{ij}\frac{\langle pa||ij\rangle F^{(1)}_{id}\langle jd||bc\rangle\langle bc||qa\rangle}{D^{\omega a}_{ij}D^{bc}_{ij}D^{d}_{i}} \quad (95)$$

and

$$K_{\alpha_{pq}}(\omega) = \frac{1}{2}\sum_{abcd}\sum_{ij}\frac{\langle pa||bc\rangle F^{(1)}_{bd}\langle dc||ij\rangle\langle ij||qa\rangle}{D^{bc}_{ij}D^{cd}_{ij}D^{\omega a}_{ij}}$$

$$K_{\beta_{pq}}(\omega) = -\frac{1}{2}\sum_{abc}\sum_{ijk}\frac{\langle pa||bc\rangle F^{(1)}_{ck}\langle bk||ij\rangle\langle ij||qa\rangle}{D^{c}_{k}D^{bc}_{ij}D^{\omega a}_{ij}}$$

$$K_{\gamma_{pq}}(\omega) = -\frac{1}{2}\sum_{abc}\sum_{ijk}\frac{\langle pa||bk\rangle F^{(1)}_{kc}\langle bc||ij\rangle\langle ij||qa\rangle}{D^{bc}_{ij}D^{\omega ac}_{ijk}D^{\omega a}_{ij}}$$

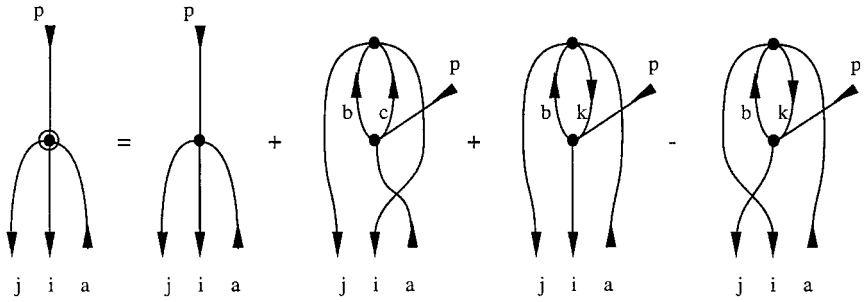

FIGURE 10. Diagrammatic expansion of the $H^{13(0)[2]}_{p,aij}$ coupling amplitude, displayed as a screened dot-vertex [14].

$$K_{\delta_{pq}}(\omega) = -\frac{1}{2}\sum_{abc}\sum_{ijk}\frac{\langle pa||bk\rangle F^{(1)}_{kc}\langle bc||ij\rangle\langle ij||qa\rangle}{D^{bc}_{ij}D^{\omega ac}_{ijk}D^{c}_{k}}, \tag{96}$$

where the energy differences are given as

$$\begin{aligned} D^{a}_{i} &= \epsilon_a - \epsilon_i \\ D^{ab}_{ij} &= \epsilon_a + \epsilon_b - \epsilon_i - \epsilon_j \\ D^{\omega a}_{ij} &= \omega + \epsilon_a - \epsilon_i - \epsilon_j \\ D^{\omega ab}_{ijk} &= \omega + \epsilon_a + \epsilon_b - \epsilon_i - \epsilon_j - \epsilon_k. \\ &\vdots \end{aligned} \tag{97}$$

In the $\mathbf{P}_\alpha$ and $\mathbf{P}_\beta$ contributions, one can easily discriminate the second-order version of the frequency-independent perturbed coupling amplitude from the first-order form of $\mathbf{H}^{ab(0)}(\omega\mathbf{1}^{bb} - \mathbf{H}^{bb(0)})^{-1}$, i.e., in this case,

$$\frac{1}{2}\sum_{ij}\frac{\langle pa||ij\rangle}{\omega + \varepsilon_a - \varepsilon_i - \varepsilon_j}. \tag{98}$$

Similarly, one can also easily extract from the $\mathbf{K}_\alpha$ and $\mathbf{K}_\beta$ contributions the first-order form of $(\omega\mathbf{1}^{bb} - \mathbf{H}^{bb(0)})^{-1}\mathbf{H}^{ba(0)}$, i.e.:

$$\frac{1}{2}\sum_{ij}\frac{\langle ij||qa\rangle}{\omega + \varepsilon_a - \varepsilon_i - \varepsilon_j}. \tag{99}$$

The remaining $\mathbf{K}_\gamma$ and $\mathbf{K}_\delta$ matrices do not allow at first glance such an easy separation. They are most conveniently merged into a single expression, from which the $(\omega\mathbf{1}^{bb} - \mathbf{H}^{bb(0)[0]})^{-1}\mathbf{H}^{ba(0)[1]}$ terms can be readily extracted, according to the following equality:

$$\frac{1}{D^{c}_{k}D^{\omega a}_{ij}} = \frac{1}{D^{\omega ac}_{ijk}D^{\omega a}_{ij}} + \frac{1}{D^{\omega ac}_{ijk}D^{c}_{k}}. \tag{100}$$

One can therefore advantageously bypass the drawing of all the third-order perturbed self-energy diagrams with a dot-vertex outside the kernel and the comparison with Eqs. (84) and (85), by considering a polarized version of the screened dot-vertices. For a consistent construction of both the **P** and **K** types of diagrams, one has to consider two sets of subgraphs, the **Π** and **Γ** series of Figures 11 and 12, obtained simply by polarizing the pending or the internal lines of the screened coupling amplitudes of Figure 10, respectively. This clearly yields the polarized screened dot-vertex required in Figure 9.

Only two time-orderings of the cross-vertex have to be considered in the first case: Any other location of the cross-vertex in the **Π** subset would be redundant with diagrams directly constructed from the screened dot-vertex, such as the **C** and **D** graphs of Figure 8. On the other hand, the **Γ** subset has to be representative of four different time-orderings. By counting all combinations which fit with a third-order form of $\mathbf{M}^{(1)}$, it is then clear that the **Π** and **Γ** series account for 40 and 48 more contributions, respectively. Translated into algebraic form, the second-order perturbed coupling amplitudes are obtained as

$$\begin{aligned} H^{13(1)[2]}_{p,aij} &= H^{13(1)[1]}_{p,aij} + \sum_{\mu=1}^{10}\Pi^{13(1)[2]}_{\mu,p,aij} + \sum_{\mu=1}^{9}\Gamma^{13(1)[2]}_{\mu,p,aij} \\ H^{13(1)[2]}_{p,iab} &= H^{13(1)[1]}_{p,iab} + \sum_{\mu=1}^{10}\Pi^{13(1)[2]}_{\mu,p,iab} + \sum_{\mu=1}^{9}\Gamma^{13(1)[2]}_{\mu,p,iab} \\ H^{31(1)[2]}_{aij,q} &= H^{13(1)[2]*}_{q,aij} \\ H^{31(1)[2]}_{iab,q} &= H^{13(1)[2]*}_{q,iab}, \end{aligned} \tag{101}$$

together with Eqs. (106)–(108) and (109) and (110) given in two appendices of this paper, where only the contributions of those contraction lines that are attached to the cross-vertex have been considered to evaluate the ''*internal*'' energy denominators of the $\mathbf{\Gamma}_7 - \mathbf{\Gamma}_9$ diagrams. This unusual rule relates to Eq. (100) and can be regarded as the final outcome of the time ambiguity arising in these diagrams with the time-ordering of the cross-vertex, with respect to the 2p–1h or 2h–1p kernels. Along the same lines, as shown in Appendix A, one can also merge into a single contribution the $\mathbf{\Pi}_1$ and $\mathbf{\Pi}_6$ terms, as well as the $\mathbf{\Pi}_5$ and $\mathbf{\Pi}_{10}$ terms.

To complete the ADC(3) expansion of the dynamic part of $\mathbf{\Sigma}^{(1)}(\omega)$, one has finally to find out all the 24 remaining third-order graphs (Figs. 13 and 14) resulting from the inclusion of the first-order form of $\mathbf{H}^{bb(1)}$ into Eqs. (92), in analogy with what has been done for ADC(2). To avoid redundancies with other diagrams, the subgraphs accounting for $\mathbf{H}^{bb(1)}$ must be displayed as a strongly connected (irreducible) form of the 2p–1h propagator, i.e., as diagrams that do not fall into disconnected parts when two particle and one hole lines (or two hole and one particle lines) are cut. As contrasted with the **P** and **K** diagrams issued from the **Π** and **Γ** subsets, these subgraphs have, furthermore, to yield a dot-vertex *inside* the kernel,

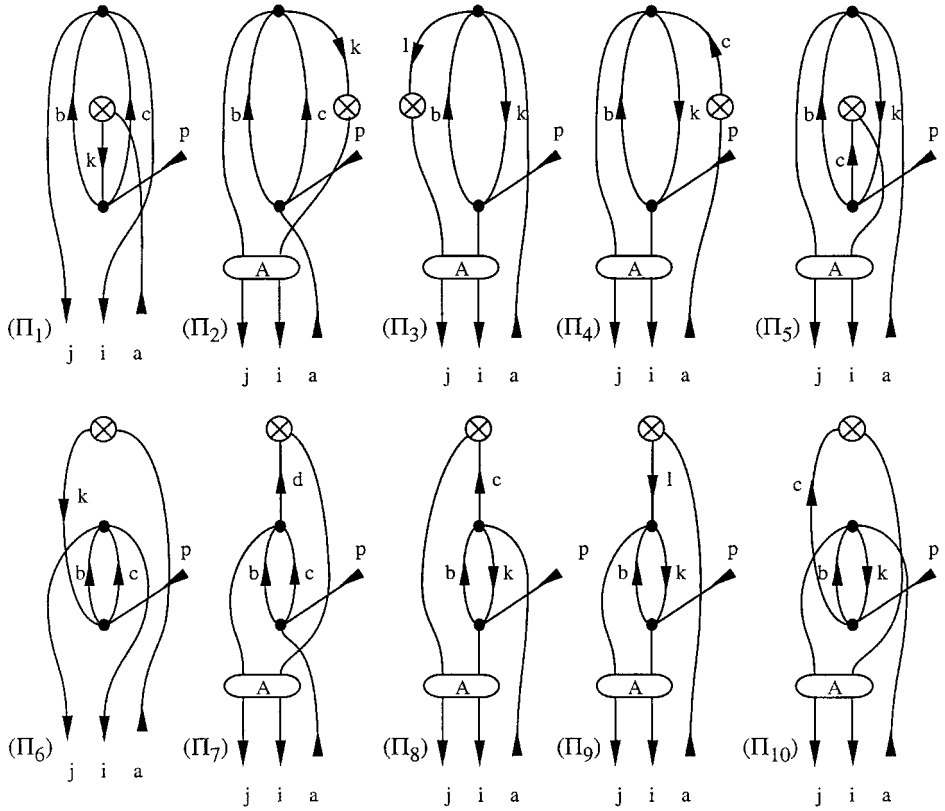

FIGURE 11. Diagrammatic expansion of the $H^{13(1)[2]}_{p,aij}$ coupling amplitude, obtained as a polarized version of Figure 10: the **Π**-terms.

such as the $\mathbf{U}_\alpha$ and $\mathbf{U}_\beta$ diagrams displayed in Figures 13 and 14, respectively. In an order-by-order expansion, however, a direct inclusion of the series of the $\mathbf{U}_\alpha$ diagrams, which are characterized by the *internal* location of the cross-vertex, would interestingly destroy the analytic structures of the perturbed self-energy, since all these terms yield third-order poles:

$$U_{1\alpha_{pq}}(\omega) = +\frac{1}{2}\sum_{ijklab}\frac{\langle pa||ij\rangle F^{(1)}_{bk}\langle ij||bl\rangle\langle kl||qa\rangle}{D^{\omega a}_{ij}D^{\omega ab}_{ijk}D^{\omega a}_{kl}}$$

$$U_{2\alpha_{pq}}(\omega) = -\sum_{ijkabc}\frac{\langle pa||ij\rangle F^{(1)}_{bk}\langle ic||ba\rangle\langle kj||qc\rangle}{D^{\omega a}_{ij}D^{\omega ab}_{ijk}D^{\omega c}_{jk}}$$

$$U_{3\alpha_{pq}}(\omega) = +\sum_{ijklab}\frac{\langle pa||ij\rangle F^{(1)}_{bk}\langle ik||la\rangle\langle lj||qb\rangle}{D^{\omega a}_{ij}D^{\omega ab}_{ijk}D^{\omega b}_{jl}}$$

$$U_{4\alpha_{pq}}(\omega) = +\frac{1}{2}\sum_{ijklab}\frac{\langle pa||kl\rangle\langle bl||ij\rangle F^{(1)}_{kb}\langle ij||qa\rangle}{D^{\omega a}_{ij}D^{\omega ab}_{ijk}D^{\omega a}_{kl}}$$

$$U_{5\alpha_{pq}}(\omega) = -\sum_{ijkabc}\frac{\langle pc||kj\rangle\langle ba||ic\rangle F^{(1)}_{kb}\langle ij||qa\rangle}{D^{\omega a}_{ij}D^{\omega ab}_{ijk}D^{\omega c}_{jk}}$$

$$U_{6\alpha_{pq}}(\omega) = +\sum_{ijklab}\frac{\langle pb||lj\rangle\langle la||ik\rangle F^{(1)}_{kb}\langle ij||qa\rangle}{D^{\omega a}_{ij}D^{\omega ab}_{ijk}D^{\omega b}_{jl}} \qquad (102)$$

To bypass this difficulty, it is again necessary to consider (Fig. 14) the set of the related $\mathbf{U}_\beta$ diagrams, differing from the $\mathbf{U}_\alpha$ diagrams only by the time-ordering of the cross-vertex, located in this case *outside* the kernel of $\mathbf{M}^{(1)}$:

$$U_{1\beta_{pq}}(\omega) = +\frac{1}{2}\sum_{ijklab}\frac{\langle pa||ij\rangle F^{(1)}_{bk}\langle ij||bl\rangle\langle kl||qa\rangle}{D^{b}_{k}D^{\omega ab}_{ijk}D^{\omega a}_{kl}}$$

$$U_{2\beta_{pq}}(\omega) = -\sum_{ijkabc}\frac{\langle pa||ij\rangle F^{(1)}_{bk}\langle ic||ba\rangle\langle kj||qc\rangle}{D^{b}_{k}D^{\omega ab}_{ijk}D^{\omega c}_{jk}}$$

$$U_{3\beta_{pq}}(\omega) = +\sum_{ijklab}\frac{\langle pa||ij\rangle F^{(1)}_{bk}\langle ij||la\rangle\langle lj||qb\rangle}{D^{b}_{k}D^{\omega ab}_{ijk}D^{\omega b}_{jl}}$$

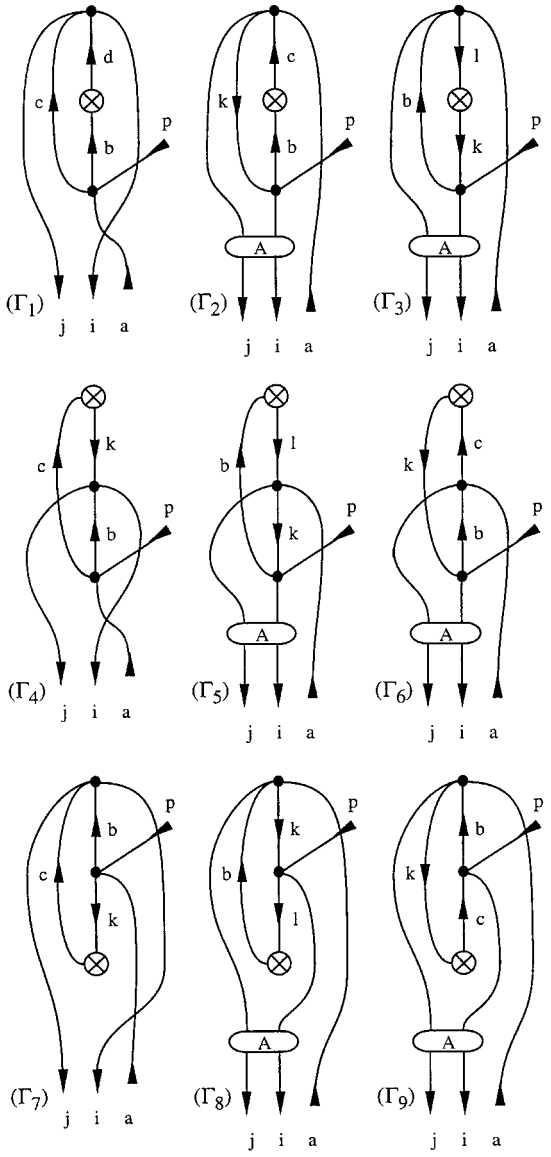

FIGURE 12. Diagrammatic expansion of the $H^{13(1)[2]}_{p,aij}$ coupling amplitude, obtained as a polarized version of Figure 10: the **Γ**-terms.

$$U_{4\beta_{pq}}(\omega) = +\frac{1}{2}\sum_{ijklab}\frac{\langle pa||kl\rangle\langle bl||ij\rangle F^{(1)}_{kb}\langle ij||qa\rangle}{D^b_k D^{\omega ab}_{ijk} D^{\omega a}_{kl}}$$

$$U_{5\beta_{pq}}(\omega) = -\sum_{ijkabc}\frac{\langle pc||kj\rangle\langle ba||ic\rangle F^{(1)}_{kb}\langle ij||qa\rangle}{D^b_k D^{\omega ab}_{ijk} D^{\omega c}_{jk}}$$

$$U_{6\beta_{pq}}(\omega) = +\sum_{ijklab}\frac{\langle pb||lj\rangle\langle la||ik\rangle F^{(1)}_{kb}\langle ij||qa\rangle}{D^b_k D^{\omega ab}_{ijk} D^{\omega b}_{jl}}. \quad (103)$$

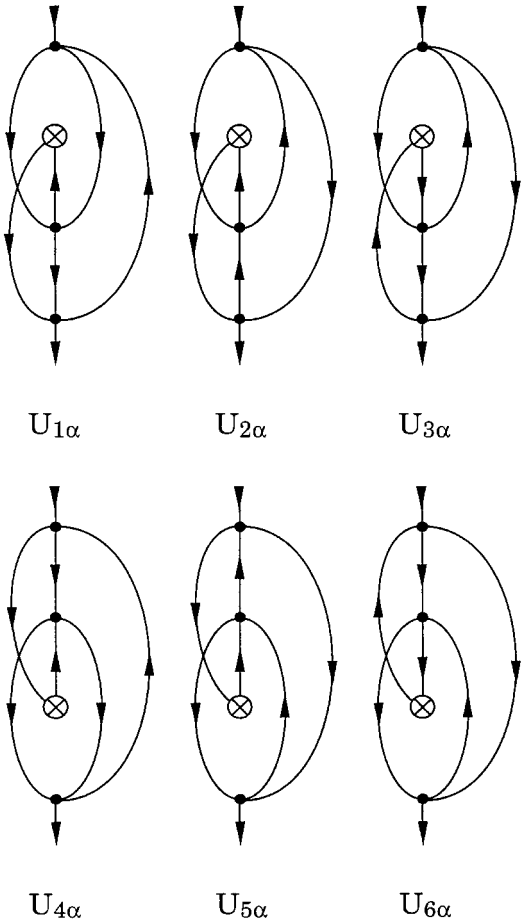

FIGURE 13. The series of the $\boldsymbol{U}_\alpha$ diagrams accounting for $\boldsymbol{H}^{bb(1)[1]}$ in the hole sector $\boldsymbol{M}^{(1)}(\omega)$.

When adding the contributions of both sets, according to Eq. (100), one obtains readily third-order perturbed self-energy expressions with second-order poles, as requested:

$$\left(U_{1\alpha}(\omega) + U_{1\beta}(\omega)\right)_{pq} = +\frac{1}{2}\sum_{ijklab}\frac{\langle pa||ij\rangle F^{(1)}_{bk}\langle ij||bl\rangle\langle kl||qa\rangle}{D^{\omega a}_{ij} D^b_k D^{\omega a}_{kl}}$$

$$\left(U_{2\alpha}(\omega) + U_{2\beta}(\omega)\right)_{pq} = -\sum_{ijkabc}\frac{\langle pa||ij\rangle F^{(1)}_{bk}\langle ic||ba\rangle\langle kj||qc\rangle}{D^{\omega a}_{ij} D^b_k D^{\omega c}_{jk}}$$

$$\left(U_{3\alpha}(\omega) + U_{3\beta}(\omega)\right)_{pq} = +\sum_{ijklab}\frac{\langle pa||ij\rangle F^{(1)}_{bk}\langle ih||la\rangle\langle lj||qb\rangle}{D^{\omega a}_{ij} D^b_k D^{\omega b}_{jl}}$$

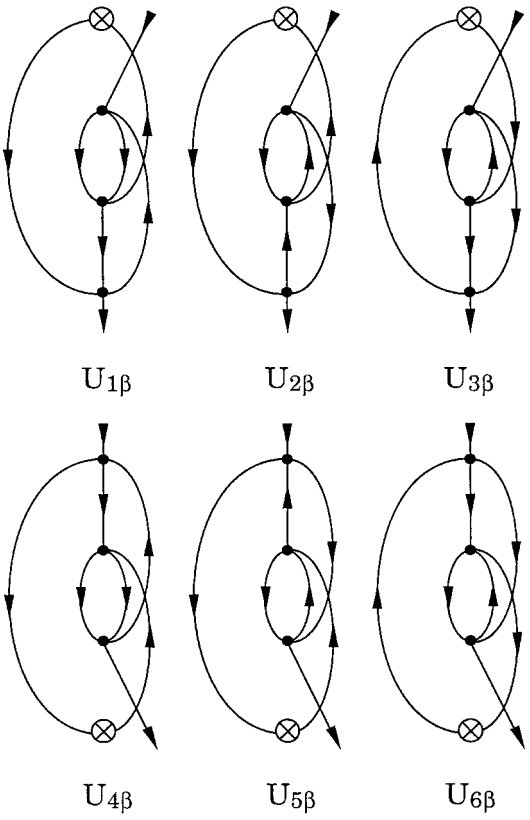

FIGURE 14. The series of the $\boldsymbol{U}_\beta$ diagrams accounting for $\boldsymbol{B}^{bb(1)[1]}$ in the hole sector of $\boldsymbol{M}^{(1)}(\omega)$.

$$\begin{aligned}
&\left(U_{4\alpha}(\omega) + U_{4\beta}(\omega)\right)_{pq} \\
&\quad = +\frac{1}{2}\sum_{ijklab} \frac{\langle pa||kl\rangle\langle bl||ij\rangle F_{kb}^{(1)}\langle ij||qa\rangle}{D_{ij}^{\omega a} D_k^b D_{kl}^{\omega a}} \\
&\left(U_{5\alpha}(\omega) + U_{5\beta}(\omega)\right)_{pq} \\
&\quad = -\sum_{ijkabc} \frac{\langle pc||kj\rangle\langle ba||ic\rangle F_{kb}^{(1)}\langle ij||qa\rangle}{D_{ij}^{\omega a} D_k^b D_{jk}^{\omega c}} \\
&\left(U_{6\alpha}(\omega) + U_{6\beta}(\omega)\right)_{pq} \\
&\quad = +\sum_{ijklab} \frac{\langle pb||lj\rangle\langle la||ik\rangle F_{kb}^{(1)}\langle ij||qa\rangle}{D_{ij}^{\omega a} D_k^b D_{jl}^{\omega b}}. \quad (104)
\end{aligned}$$

On these considerations, one can than easily draw and evaluate all the first-order ''time-merged'' contributions to the hexagon-cluster (Fig. 15). The first-order clusters $\boldsymbol{\Delta}_1$ to $\boldsymbol{\Delta}_6$ can be directly compared to the diagrammatic structures contained within the kernel of the $\mathbf{U}_1$–$\mathbf{U}_6$ diagrams of Figure 13. As usual, one has to count the number of topological degeneracies, hole lines, and closed fermion loops that are added when inserting these structures into the generic diagrams of Figure 7 to evaluate their sign and weight factor. As for the $\boldsymbol{\Gamma}_7$–$\boldsymbol{\Gamma}_9$ graphs, one has also to consider only the contributions of the contraction lines attached to the cross-vertex to evaluate the energy denominators. This again can be related to the fact that each of the $\boldsymbol{\Delta}$-clusters account for two different locations of the cross-vertex, inside and outside the kernels. By means of these rules, the $\mathbf{H}_{bb}^{(1)}$ matrix is therefore easily and consistently expanded up to first-order in correlation, as

$$\begin{aligned}
H_{ija,i'j'a'}^{33(1)[1]} &= H_{ija,i'j'a'}^{33(1)[0]} + \sum_{\mu=1}^{6} \Delta_{\mu,ija,i'j'a'}^{2h-1p} \\
H_{abi,a'b'i'}^{33(1)[1]} &= H_{abi,a'b'i'}^{33(1)[0]} + \sum_{\mu=1}^{6} \Delta_{\mu,abi,a'b'i'}^{2h-1p},
\end{aligned} \quad (105)$$

together with Eqs. (111) and (112) given in the third appendix of this article.

Here, again, the consistency of the direct diagrammatic approach can be easily assessed by inserting into Eq. (92) the expressions corresponding to the $\boldsymbol{\Delta}_1$–$\boldsymbol{\Delta}_6$ clusters belonging to the 2h–1p configuration subspace and comparing successively the expressions obtained to each of the third-order perturbed self-energy terms in Eqs. (104).

Besides the dynamic part $\mathbf{M}^{(1)}(\omega)$ of the perturbed self-energy, one should also consider at third-order in electronic correlation the constant component $\Sigma(s)$ relating to the second-order correlation form of the perturbed one-electron density, according to Eq. (89). As shown previously [41], the coupled perturbed one-electron density can be sorted out into ''dynamic'' and ''static'' parts, relating to the perturbed dynamic self-energy and to the perturbed Fock matrix, respectively. As the second-order perturbed one-electron density amounts to 96 different terms, it will also clearly yield the 96 topologically distinct time-ordered irreducible diagrams that are required for $\boldsymbol{\Sigma}^{(1)[3]}(\infty)$. The constant part of $\boldsymbol{\Sigma}^{(1)[3]}$ can therefore be readily expanded using the expressions derived in [41] for $\boldsymbol{\rho}_1^{(1)[2]}$.

In analogy with the constant part of the unperturbed self-energy [18], one can expect a logarithmic size-dependence for those $\boldsymbol{\Sigma}^{(1)[3]}(\infty)$ terms that are related to the 30 $\boldsymbol{\rho}_1^{(1)[2]}$ densities contributing to the particle number, through the interplay of their trace [41]. As shown in [41], the gauge invariance

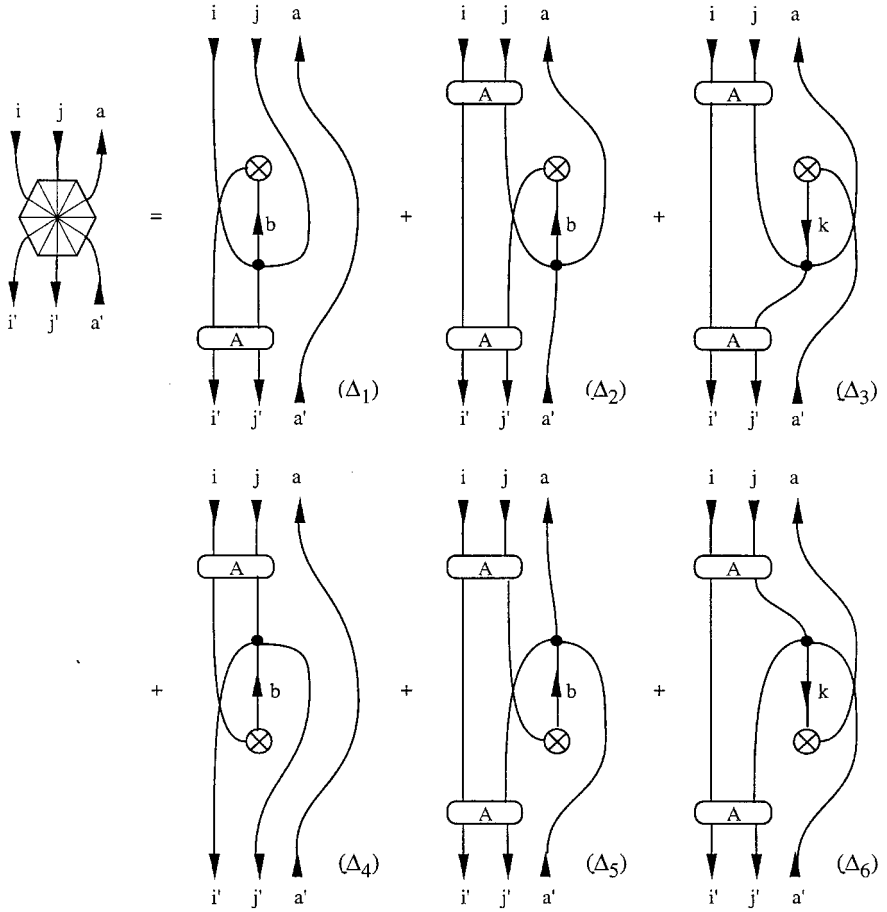

FIGURE 15. The six time-merged kernels contributing to the $H^{33(1)[1]}_{ija,i'j'a'}$ coupling amplitude, in one-to-one correspondence with the $\boldsymbol{M}^{(1)[3]}$ diagrams of Figure 13 and 14.

of linear response properties is ensured in second-order coupled electron propagator calculations by a strict cancellation of the successive contributions to $tr[\boldsymbol{\rho}_1^{(1)[2]}]$. Accordingly, from the arguments developed in [18], one can also expect a strict cancellation of the logarithmic behaviors of the diverging $\boldsymbol{\Sigma}^{(1)[3]}(\infty)$ terms, ensuring the requested size-intensive scaling of the residue.

Conclusions

The coupled perturbed one-electron propagator can be advantageously used to incorporate high-order correlation corrections in the computation of linear and quadratic responses, through the interlay of the first-order perturbed forms of the one-electron density and self-energy, $\boldsymbol{\rho}_1^{(1)}$ and $\boldsymbol{\Sigma}^{(1)}(\omega)$, respectively. In this study, we derived new schemes by means of an algebraic diagrammatic construction to expand consistently $\boldsymbol{\Sigma}^{(1)}(\omega)$ *through* second order and third order in correlation. The obtained CPEP/ADC(3) equations provide the very first approach for the computation of molecular responses at a level equivalent to a third-order polarization propagator expansion, a virtually intractable approximation which would require the inclusion of 2160 terms in the diagrammatic perturbation series accounting for this propagator.

As for the first-order part of the perturbed one-electron propagator, $\mathbf{G}_1^{(1)}(\omega)$, an exact form of the dynamic part $\mathbf{M}^{(1)}(\omega)$ of the perturbed self-energy yields single and quadratic poles. As $\boldsymbol{\rho}_1^{(1)}$ is obtained by contour integration along the Coulson contour, its quality is essentially determined by the residues at the poles of $\mathbf{G}_1^{(1)}(\omega)$. For accurate results, therefore, it is essential to find self-energy approximations exhibiting the same analytical structure as $\boldsymbol{\Sigma}^{(1)}(\omega)$. A direct inclusion of the 192 terms accounting for the dynamic part of the

third-order perturbed self-energy would not only be completely out of range in practice, it should also be regarded with exceedingly great caution since 36 of the terms to be included yield third-order poles, in terms of a Laurent expansion.

In this derivation, appropriate ''macrodiagrams'' have been introduced to bypass the comparison procedure between all the terms contributing to $\mathbf{M}^{(1)[2]}$ and $\mathbf{M}^{(1)[3]}$ with the analytic form required for the dynamic part of the perturbed self-energy. Besides a straightforward transcription of the parts of diagrams and thereby collective esccitations of interest into matrix equations, this direct diagrammatic construction also enables some physical insight. In the ADC schemes, third and higher orders can be attained by means of a 2ph-TDA renormalization, which preserves the analytical structure of $\mathbf{\Sigma}^{(1)}(\omega)$. This renormalization implies that infinite geometric series of diagrams and thereby collective excitations of mixed RPA-ladder type are automatically included, by virtue of a Born expansion of matrix inverses. Both the ADC(2) [2ph-TDA] and ADC(3) [extended 2ph-TDA] schemes account for the polarization of the 2p−1h and 2h−1p linear responses and bielectron interactions under an external field. The extended 2ph-TDA scheme also accounts, through the interplay of the coupling amplitudes, for a first-order screening of the external field and bielectron interactions by the effects of electronic correlation in the ground state.

A major advantage of the CPEP/ADC(2) or CPEP/ADC(3) schemes in comparison with equivalent methods based on the polarization propagator, respectively, SOPPA and TOPPA (second-order and third-order polarization propagator approaches), is the particle rank (h_3 vs. h_4) of the effective energy interaction matrix which has to be inverted. The price to pay for it is, as in a coupled perturbed Hartree−Fock scheme, the iteration for the perturbed density, which itself can be efficiently computed [23] using numerical quadrature in the complex ω-plane. As it is always possible to detach the external perturbation from the frequency-dependent CPEP kernels, the expensive parts for the accumulation in the quadrature only need to be calculated once in practice, at the cost of making them 4-index quantities in terms of the MO basis. As contrasted with the 192 terms needed to evaluate $\mathbf{M}^{(1)[3]}(\omega)$, the compactness of the ADC(3) scheme appears also as a decisive advantage: only 4, 34, and 12 terms are effectively needed to evaluate the required coupling amplitudes, $\mathbf{H}^{ab(0)[2]}$, $\mathbf{H}^{ab(1)[2]}$, and $\mathbf{H}^{bb(1)[1]}$, respectively.

Although at the third-order level in correlation the constant part of the self-energy, $\mathbf{\Sigma}^{(1)[3]}(\infty)$, also accounts for 96 different contributions, it does not, in practice, lead really to additional computational constraints, since it can be readily evaluated from the second-order form of the perturbed electron density. On the other hand, numerical errors in the computed densities could yield a slight violation of the particle number, implying at the third-order level in correlation the loss of both gauge invariance and size-extensivity for the computed linear responses. For similar reasons, a renormalization of $\boldsymbol{\rho}_1^{(1)}$ through the interplay of the dynamic self-energies would also lead to a loss of gauge invariance and size-extensivity. Research is under progress in the Sheffield group to limit these deficiencies.

Appendix A: The Π Terms

$$\Pi^{13(1)[2]}_{1,\,p,\,aij} = -\frac{1}{2} \times \sum_{bck} \frac{F^{(1)}_{ak}\langle\, pk||bc\rangle\langle\, bc||ij\rangle}{(\varepsilon_i+\varepsilon_j-\varepsilon_b-\varepsilon_c)(\varepsilon_i+\varepsilon_j+\varepsilon_k-\varepsilon_a-\varepsilon_b-\varepsilon_c)}$$

$$\Pi^{13(1)[2]}_{2,\,p,\,aij} = -\frac{1}{2}(1-P_{ij}) \times \sum_{bck} \frac{\langle\, pa||bc\rangle\langle\, bc||kj\rangle F^{(1)}_{ki}}{(\varepsilon_j+\varepsilon_k-\varepsilon_b-\varepsilon_c)(\varepsilon_i+\varepsilon_j-\varepsilon_b-\varepsilon_c)}$$

$$\Pi^{13(1)[2]}_{3,\,p,\,aij} = +(1-P_{ij}) \times \sum_{bkl} \frac{\langle\, pk||bi\rangle\langle\, ab||kl\rangle F^{(1)}_{ij}}{(\varphi_k+\varepsilon_l-\varepsilon_a-\varepsilon_b)(\varepsilon_j+\varepsilon_k-\varepsilon_a-\varepsilon_b)}$$

$$\Pi^{13(1)[2]}_{4,\,p,\,aij} = -(1-P_{ij}) \times \sum_{bck} \frac{\langle\, pk||bi\rangle F^{(1)}_{ac}\langle\, bc||jk\rangle}{(\varepsilon_j+\varepsilon_k-\varepsilon_b-\varepsilon_c)(\varepsilon_j+\varepsilon_k-\varepsilon_a-\varepsilon_b)}$$

$$\Pi^{13(1)[2]}_{5,\,p,\,aij} = -(1-P_{ij}) \times \sum_{bck} \frac{\langle\, pk||bc\rangle F^{(1)}_{ci}\langle\, ba||jk\rangle}{(\varepsilon_j+\varepsilon_k-\varepsilon_a-\varepsilon_b)(\varepsilon_i+\varepsilon_j+\varepsilon_k-\varepsilon_a-\varepsilon_b-\varepsilon_c)}$$

$$\Pi^{13(1)[2]}_{6,p,aij} = -\frac{1}{2} \times \sum_{bck} \frac{F^{(1)}_{ak}\langle pk||bc\rangle\langle bc||ij\rangle}{(\varepsilon_i+\varepsilon_j+\varepsilon_k-\varepsilon_a-\varepsilon_b-\varepsilon_c)(\varepsilon_k-\varepsilon_a)}$$

$$\Pi^{13(1)[2]}_{7,p,aij} = +\frac{1}{2}(1-P_{ij}) \times \sum_{bck} \frac{\langle pa||bc\rangle\langle bc||dj\rangle F^{(1)}_{di}}{(\varepsilon_i-\varepsilon_d)(\varepsilon_i+\varepsilon_j-\varepsilon_b-\varepsilon_c)}$$

$$\Pi^{13(1)[2]}_{8,p,aij} = -(1-P_{ij}) \times \sum_{bck} \frac{\langle pk||bi\rangle\langle ab||kc\rangle F^{(1)}_{cj}}{(\varepsilon_j-\varepsilon_c)(\varepsilon_j+\varepsilon_k-\varepsilon_a-\varepsilon_b)}$$

$$\Pi^{13(1)[2]}_{9,p,aij} = +(1-P_{ij}) \times \sum_{bkl} \frac{\langle pk||bi\rangle F^{(1)}_{al}\langle bl||jk\rangle}{(\varepsilon_l-\varepsilon_a)(\varepsilon_j+\varepsilon_k-\varepsilon_a-\varepsilon_b)}$$

$$\Pi^{13(1)[2]}_{10,p,aij} = -(1-P_{ij}) \times \sum_{bck} \frac{\langle pk||bc\rangle F^{(1)}_{ci}\langle ba||jk\rangle}{(\varepsilon_i-\varepsilon_c)(\varepsilon_i+\varepsilon_j+\varepsilon_k-\varepsilon_a-\varepsilon_b-\varepsilon_c)}. \quad (106)$$

Some of these terms can be merged together as

$$\Pi^{13(1)[2]}_{1+6,p,aij} = -\frac{1}{2}\sum_{bck} F^{(1)}_{ak}\frac{\langle pk||bc\rangle\langle bc||ij\rangle}{(\varepsilon_i+\varepsilon_j-\varepsilon_a-\varepsilon_b)(\varepsilon_k-\varepsilon_a)}$$

$$\Pi^{13(1)[2]}_{5+10,p,aij} = -(1-P_{ij}) \times \sum_{bck} \frac{\langle pk||bc\rangle F^{(1)}_{ci}\langle ba||jk\rangle}{(\varepsilon_i-\varepsilon_c)(\varepsilon_j+\varepsilon_k-\varepsilon_a-\varepsilon_b)}. \quad (107)$$

Similarly,

$$\Pi^{13(1)[2]}_{1+6,p,aib} = +\frac{1}{2}\sum_{ckj} \frac{F^{(1)}_{ic}\langle pc||jk\rangle\langle jk||ab\rangle}{(\varepsilon_j+\varepsilon_k-\varepsilon_a-\varepsilon_b)(\varepsilon_i-\varepsilon_c)}$$

$$\Pi^{13(1)[2]}_{2,p,aib} = +\frac{1}{2}(1-P_{ab}) \times \sum_{ckj} \frac{\langle pi||jk\rangle\langle jk||cb\rangle F^{(1)}_{ca}}{(\varepsilon_j+\varepsilon_k-\varepsilon_a-\varepsilon_b)(\varepsilon_j+\varepsilon_k-\varepsilon_b-\varepsilon_c)}$$

$$\Pi^{13(1)[2]}_{3,p,aib} = -(1-P_{ab}) \times \sum_{cdj} \frac{\langle pc||ja\rangle\langle ji||dc\rangle F^{(1)}_{db}}{(\varepsilon_i+\varepsilon_j-\varepsilon_b-\varepsilon_c)(\varepsilon_i+\varepsilon_j-\varepsilon_c-\varepsilon_d)}$$

$$\Pi^{13(1)[2]}_{4,p,aib} = +(1-P_{ab}) \times \sum_{ckj} \frac{\langle pc||ja\rangle F^{(1)}_{ik}\langle jk||bc\rangle}{(\varepsilon_i+\varepsilon_j-\varepsilon_b-\varepsilon_c)(\varepsilon_j+\varepsilon_k-\varepsilon_b-\varepsilon_c)}$$

$$\Pi^{13(1)[2]}_{5+10,p,aib} = +(1-P_{ab}) \times \sum_{ckj} \frac{\langle pc||jk\rangle F^{(1)}_{ka}\langle ji||bc\rangle}{(\varepsilon_i+\varepsilon_j-\varepsilon_b-\varepsilon_c)(\varepsilon_k-\varepsilon_a)}$$

$$\Pi^{13(1)[2]}_{7,p,aib} = -\frac{1}{2}(1-P_{ab}) \times \sum_{jkl} \frac{\langle pi||jk\rangle\langle jk||lb\rangle F^{(1)}_{la}}{(\varepsilon_j+\varepsilon_k-\varepsilon_a-\varepsilon_b)(\varepsilon_l-\varepsilon_a)}$$

$$\Pi^{13(1)[2]}_{8,p,aib} = +(1-P_{ab}) \times \sum_{ckj} \frac{\langle pc||ja\rangle\langle ji||kc\rangle F^{(1)}_{kb}}{(\varepsilon_i+\varepsilon_j-\varepsilon_b-\varepsilon_c)(\varepsilon_k-\varepsilon_b)}$$

$$\Pi^{13(1)[2]}_{9,p,aib} = -(1-P_{ab}) \times \sum_{cdj} \frac{\langle pc||ja\rangle F^{(1)}_{id}\langle jd||bc\rangle}{(\varepsilon_i+\varepsilon_j-\varepsilon_b-\varepsilon_c)(\varepsilon_d-\varepsilon_i)}. \quad (108)$$

Appendix B: The Γ Terms

$$\Gamma^{13(1)[2]}_{1,p,aij} = +\sum_{bcd} \frac{\langle pa||bc\rangle F^{(1)}_{bd}\langle dc||ij\rangle}{(\varepsilon_i+\varepsilon_j-\varepsilon_b-\varepsilon_c)(\varepsilon_i+\varepsilon_j-\varepsilon_c-\varepsilon_d)}$$

$$\Gamma^{13(1)[2]}_{2,p,aij} = -(1-P_{ij}) \times \sum_{bck} \frac{\langle pk||bi\rangle F^{(1)}_{bc}\langle ac||kj\rangle}{(\varepsilon_j+\varepsilon_k-\varepsilon_a-\varepsilon_b)(\varepsilon_j+\varepsilon_k-\varepsilon_a-\varepsilon_c)}$$

$$\Gamma^{13(1)[2]}_{3,p,aij} = +(1-P_{ij}) \times \sum_{bkl} \frac{\langle pk||bi\rangle F^{(1)}_{lk}\langle ab||lj\rangle}{(\varepsilon_j+\varepsilon_k-\varepsilon_a-\varepsilon_b)(\varepsilon_j+\varepsilon_l-\varepsilon_a-\varepsilon_b)}$$

$$\Gamma^{13(1)[2]}_{4,p,aij} = -\sum_{bck} \frac{\langle pa||bc\rangle F^{(1)}_{ck}\langle bk||ij\rangle}{(\varepsilon_k-\varepsilon_c)(\varepsilon_i+\varepsilon_j-\varepsilon_b-\varepsilon_c)}$$

$$\Gamma^{13(1)[2]}_{5,p,aij} = +(1-P_{ij}) \times \sum_{bkl} \frac{\langle pk||bi\rangle F^{(1)}_{bl}\langle al||kj\rangle}{(\varepsilon_l-\varepsilon_b)(\varepsilon_j+\varepsilon_k-\varepsilon_a-\varepsilon_b)}$$

$$\Gamma^{13(1)[2]}_{6,p,aij} = -(1-P_{ij})\sum_{bck} \frac{\langle pk||bi\rangle F^{(1)}_{ck}\langle ab||cj\rangle}{(\varepsilon_k-\varepsilon_c)(\varepsilon_j+\varepsilon_k-\varepsilon_a-\varepsilon_b)}$$

$$\Gamma^{13(1)[2]}_{7,p,aij} = -\sum_{bck} \frac{\langle pa||bk\rangle F^{(1)}_{kc}\langle bc||ij\rangle}{(\varepsilon_k-\varepsilon_c)(\varepsilon_i+\varepsilon_j-\varepsilon_b-\varepsilon_c)}$$

$$\Gamma^{13(1)[2]}_{8,p,aij} = (1-P_{ij})\sum_{bkl} \frac{\langle pk||li\rangle F^{(1)}_{lb}\langle ab||kj\rangle}{(\varepsilon_l-\varepsilon_b)(\varepsilon_j+\varepsilon_k-\varepsilon_a-\varepsilon_b)}$$

$$\Gamma^{13(1)[2]}_{9,p,aij} = -(1-P_{ij}) \times \sum_{bck} \frac{\langle pc||bi\rangle F^{(1)}_{kc}\langle ab||kj\rangle}{(\varepsilon_k-\varepsilon_c)(\varepsilon_j+\varepsilon_k-\varepsilon_a-\varepsilon_b)} \tag{109}$$

$$\Gamma^{13(1)[2]}_{1,p,aib} = -\sum_{jkl} \frac{\langle pi||jk\rangle F^{(1)}_{jl}\langle lk||ab\rangle}{(\varepsilon_j+\varepsilon_k-\varepsilon_a-\varepsilon_b)(\varepsilon_k+\varepsilon_l-\varepsilon_a-\varepsilon_b)}$$

$$\Gamma^{13(1)[2]}_{2,p,aib} = +(1-P_{ab}) \times \sum_{ckj} \frac{\langle pc||ja\rangle F^{(1)}_{jk}\langle ki||bc\rangle}{(\varepsilon_i+\varepsilon_j-\varepsilon_b-\varepsilon_c)(\varepsilon_i+\varepsilon_k-\varepsilon_b-\varepsilon_c)}$$

$$\Gamma^{13(1)[2]}_{3,p,aib} = -(1-P_{ab}) \times \sum_{cdj} \frac{\langle pc||ja\rangle F^{(1)}_{dc}\langle ij||db\rangle}{(\varepsilon_i+\varepsilon_j-\varepsilon_b-\varepsilon_c)(\varepsilon_i+\varepsilon_j-\varepsilon_b-\varepsilon_d)}$$

$$\Gamma^{13(1)[2]}_{4,p,aib} = +\sum_{ckj} \frac{\langle pi||jk\rangle F^{(1)}_{kc}\langle jc||ab\rangle}{(\varepsilon_k-\varepsilon_c)(\varepsilon_j+\varepsilon_k-\varepsilon_a-\varepsilon_b)}$$

$$\Gamma^{13(1)[2]}_{5,p,aib} = -(1-P_{ab}) \times \sum_{cdj} \frac{\langle pc||ja\rangle F^{(1)}_{jk}\langle di||bc\rangle}{(\varepsilon_j-\varepsilon_d)(\varepsilon_i+\varepsilon_j-\varepsilon_b-\varepsilon_c)}$$

$$\Gamma^{13(1)[2]}_{6,p,aib} = +(1-P_{ab}) \times \sum_{ckj} \frac{\langle pc||ja\rangle F^{(1)}_{kc}\langle ij||kb\rangle}{(\varepsilon_k-\varepsilon_c)(\varepsilon_i+\varepsilon_j-\varepsilon_b-\varepsilon_c)}$$

$$\Gamma^{13(1)[2]}_{7,p,aib} = +\sum_{ckj} \frac{\langle pi||jc\rangle F^{(1)}_{ck}\langle jk||ab\rangle}{(\varepsilon_k-\varepsilon_c)(\varepsilon_j+\varepsilon_k-\varepsilon_a-\varepsilon_b)}$$

$$\Gamma^{13(1)[2]}_{8,p,aib} = -(1-P_{ab}) \times \sum_{cdj} \frac{\langle pc||da\rangle F^{(1)}_{dj}\langle ji||bc\rangle}{(\varepsilon_j-\varepsilon_d)(\varepsilon_i+\varepsilon_j-\varepsilon_b-\varepsilon_c)}$$

$$\Gamma^{13(1)[2]}_{9,p,aib} = +(1-P_{ab}) \times \sum_{ckj} \frac{\langle pk||ja\rangle F^{(1)}_{ck}\langle ij||cb\rangle}{(\varepsilon_k-\varepsilon_c)(\varepsilon_i+\varepsilon_j-\varepsilon_b-\varepsilon_c)}. \tag{110}$$

Appendix C: The Δ Terms

To first order in correlation, and from the diagrams displayed in Figure 13, one finds

$$\Delta^{2h-1p}_{1ija,i'j'a'} = -\delta_{aa'}(1-P_{i'j'})\sum_b \frac{F^{(1)}_{bi'}\langle ij||bj'\rangle}{(\varepsilon_b-\varepsilon_{i'})}$$

$$\Delta^{2h-1p}_{2ija,i'j'a'} = (1-P_{ij})(1-P_{i'j'})\delta_{ii'}\sum_b \frac{F^{(1)}_{bj}\langle ja'||ba\rangle}{(\varepsilon_b-\varepsilon_{j'})}$$

$$\Delta^{2h-1p}_{3ija,i'j'a'} = (1-P_{ij})(1-P_{i'j'})\delta_{ii'}\sum_k \frac{F^{(1)}_{a'k}\langle jk||j'a\rangle}{(\varepsilon_{a'}-\varepsilon_k)}$$

$$\Delta^{2h-1p}_{4ija,i'j'a'} = -\delta_{aa'}(1-P_{ij})\sum_b \frac{F^{(1)}_{ib}\langle bj||i'j'\rangle}{(\varepsilon_b-\varepsilon_i)}$$

$$\Delta^{2h-1p}_{5ija,i'j'a'} = (1-P_{ij})(1-P_{i'j'})\delta_{ii'}\sum_b \frac{F^{(1)}_{jb}\langle ba'||j'a\rangle}{(\varepsilon_b-\varepsilon_j)}$$

$$\Delta^{2h-1p}_{6ija,i'j'a'} = -(1-P_{ij})(1-P_{i'j'})\delta_{ii'} \times \sum_k \frac{F^{(1)}_{ka}\langle ja'||j'k\rangle}{(\varepsilon_a-\varepsilon_k)} \tag{111}$$

for the perturbed coupling amplitudes defined in the h_3 shake-up configuration subspace and

$$\Delta^{2p-1h}_{1abi,a'b'i'} = -\delta_{ii'}(1-P_{a'b'})\sum_j \frac{F^{(1)}_{ja'}\langle ab||jb'\rangle}{(\varepsilon_j-\varepsilon_{a'})}$$

$$\Delta^{2p-1h}_{2abi,a'b'i'} = (1-P_{ab})(1-P_{a'b'})\delta_{aa'} \times \sum_j \frac{F^{(1)}_{jb'}\langle bi'||ji\rangle}{(\varepsilon_j-\varepsilon_{b'})}$$

$$\Delta^{2p-1h}_{3abi,a'b'i'} = -(1-P_{ab})(1-P_{a'b'})\delta_{aa'} \times \sum_c \frac{F^{(1)}_{i'c}\langle bc||b'i\rangle}{(\varepsilon_{i'}-\varepsilon_c)}$$

$$\Delta^{2p-1h}_{4abi,a'b'i'} = -\delta_{ii'}(1-P_{ab})\sum_j \frac{F^{(1)}_{aj}\langle jb||a'b'\rangle}{(\varepsilon_j-\varepsilon_a)}$$

$$\Delta^{2p-1h}_{5abi,a'b'i'} = (1-P_{ab})(1-P_{a'b'})\delta_{aa'} \times \sum_j \frac{F^{(1)}_{bj}\langle ji'||b'i\rangle}{(\varepsilon_j-\varepsilon_b)}$$

$$\Delta^{2p-1h}_{6abi,a'b'i'} = -(1-P_{ab})(1-P_{a'b'})\delta_{aa'} \times \sum_c \frac{F^{(1)}_{ci}\langle bi'||b'c\rangle}{(\varepsilon_i-\varepsilon_c)} \qquad (112)$$

for the perturbed coupling amplitudes defined in the h_3 shake-on configuration subspace.

ACKNOWLEDGMENTS

M. Deleuze is grateful to the FNRS, the Belgian National Fund for Scientific Research, for his former position as a Senior Research Assistant for the former laboratoire de Chimie Théorique Appliquée at the Facultés Universitaires Notre-Dame de la Paix (FUNDP), Namur (Belgium). He is indebted to Professors J. Schirmer and L. S. Cederbaum for generous hospitality, critical reading, and useful discussions about Green's functions at the Institut für Physikalische Chemie, Theoretische Chemie, Universität Heidelberg (Germany), where a part of this derivation was completed. The authors would like to express their gratitude to Professor J. Delhalle for continuous support and collaboration at the former Laboratoire de Chimie Théorique Appliquée at the Facultés Universitaires Notre-Dame de la Paix (FUNDP), Namur (Belgium).

References

1. A. L. Fetter and J. D. Walecka, *Quantum Theory of Many Particle Systems* (McGraw-Hill, New York, 1971).
2. J. Linderberg and Y. Öhrn, *Propagators in Quantum Chemistry* (Academic Press, New York, 1973).
3. L. S. Cederbaum and W. Domcke, Adv. Chem. Phys. **36**, 205 (1977).
4. (a) Y. Öhrn and G. Born, Adv. Quantum Chem. **13**, 1 (1981); (b) W. Von Niessen, J. Schirmer, and L. S. Cederbaum, Comput. Phys. Rep. **1**, 57 (1984); (c) L. S. Cederbaum, W. Domcke, J. Schirmer, and W. Von Niessen, Adv. Chem. Phys. **65**, 115 (1986).
5. J.-L. Calais, B. T. Pickup, M. Deleuze, and J. Delhalle, Eur. J. Phys. **16**, 179 (1995).
6. (a) L. J. Holleboom, J. G. Snijders, and E. J. Baerends, Int. J. Quantum Chem. **34**, 289 (1988); (b) L. J. Holleboom and J. G. Snijders, Int. J. Quantum Chem., **43**, 259 (1992); (c) J. V. Ortiz, Int. J. Quantum Chem. **S26** 1 (1992).
7. L. J. Holleboom, J. G. Snijders, E. J. Baerends, and N. A. Buijse, J. Chem. Phys. **89**, 8638 (1988).
8. G. Y. Csanak and H. S. Taylor, Adv. At. Mol. Phys. **7**, 287 (1971).
9. M. Berman, O. Walter, and L. S. Cederbaum, Phys. Rev. Lett. **50**, 1979 (1983).
10. (a) B. T. Pickup, Chem. Phys. **19**, 193 (1977); (b) M. Deleuze, B. T. Pickup, and J. Delhalle, Mol. Phys. **83**, 655 (1994).
11. (a) J. Oddershede, Adv. Quantum Chem. **11**, 275 (1978); (b) J. Oddershede, P. Jørgensen, and D. Yeager, Comp. Phys. Rep. **2**, 33 (1984); (c) J. Oddershede, Adv. Quantum Chem. **69**, 201 (1987); (d) J. Oddershede, in *Methods in Computational Molecular Physics*, G. H. F. Diercksen and S. Wilson, Eds. (Plenum Press, New York, 1992), p. 103.
12. D. N. Zubarev, Fiz. Nauk. **71**, 71 (1960); *Ibid*., Engl. Trans., Sov. Phys. Usp. **3**, 320 (1960).
13. J. Schirmer, Phys. Rev. A **43**, 4647 (1991).
14. M. Deleuze, PhD Thesis, FUNDP-Namur, Belgium, 1993).
15. M. Deleuze, J. Delhalle, B. T. Pickup, and J.-L. Calais, Adv. Quantum Chem. **26**, 35 (1995).
16. (a) M. Deleuze, J. Delhalle, and J.-M. André, Int. J. Quantum Chem. **41**, 243; (1992); (b) M. Deleuze, J. Delhalle, B. T. Pickup, and J.-L. Calais, Phys. Rev. B **46**, 15668 (1992).
17. M. Deleuze, and B. T. Pickup, J. Chem. Phys. **102**, 8967 (1995).
18. M. Deleuze, M. K. Scheller, and L. S. Cederbaum, J. Chem. Phys. **103**, 3578 (1995).
19. (a) J. Goldstone, Proc. R. Soc. Lond. A **239**, 267 (1957); (b) J. Paldus and J. Cisek, Adv. Quantum Chem. **7**, 105 (1975); V. Kvanicka, Adv. Chem. Phys. **36**, 345 (1977).
20. N. H. March, W. H. Young, and S. Sampanthar, *The Many-Body Problem in Quantum Mechanics* (Cambridge University Press, Cambridge, 1967).
21. A. D. Buckingham, Adv. Chem. Phys. **12**, 107 (1967).
22. W. Fowler, Annu. Rep. Chem. Soc. Sect C **84**, 3 (1987).
23. (a) B. T. Pickup, Int. J. Quantum Chem. Symp. **26**, 13 (1992); (b) B. T. Pickup, Philos. Mag. B **69**, 799 (1994).
24. G. H. F. Diercksen, and R. McWeeny, J. Chem. Phys. **44**, 3554 (1966); R. McWeeny and G. H. F. Diercksen, J. Chem. Phys. **49**, 4852 (1969).

25. A. D. McClachlan and M. A. Ball, Rev. Mod. Phys. **36**, 884 (1964); *Ibid*., Mol. Phys. **7**, 501 (1964); D. J. Rowe, Rev. Mod. Phys. **40**, 153 (1968).
26. B. T. Pickup et al., to be published.
27. A. D. Mattuck, *A Guide to Feynman Diagrams in the Many-Body Problem* (McGraw-Hill, New York, 1967).
28. B. T. Pickup and O. Goscinski, Mol. Phys. **26**, 1013 (1973).
29. D. J. Rowe, Rev. Mod. Phys. **40**, 153 (1968).
30. R. Manne, Int. J. Quantum Chem. **S11**, 175 (1977); R. Manne, Chem. Phys. Lett. **45**, 470 (1977); E. Dalgaard, Int. J. Quantum Chem. **15** 169 (1979).
31. J. Baker and B. T. Pickup, Chem. Phys. Lett. **56**, 537 (1980).
32. J. Baker, Chem. Phys. **79**, 117 (1983).
33. J. Schirmer and L. S. Cederbaum, J. Phys. B, **11**, 1889 (1978).
34. O. Walter and J. Schirmer, J. Phys. B **14**, 3805 (1981).
35. J. Schirmer, L. S. Cederbaum, and O. Walter, Phys. Rev. A **28**, 1237 (1983).
36. (a) J. Schirmer, Phys. Rev. A **26**, 2395 (1981); (b) J. Schirmer and A. Barth, Z. Phys. A **137**, 267 (1984).
37. J. Oddershede and P. Jørgensen, J. Chem. Phys. **66**, 1541 (1977).
38. J. Schirmer, Phys. Rev. A **26**, 2395 (1982).
39. K. Arita and P. Horie, Nucl. Phys. A **173**, 97 (1971).
40. (a) A. Trofimov and J. Schirmer, J. Phys. B **28**, 2299 (1995); (b) A. Trofimov and J. Schirmer, submitted.
41. M. Deleuze, M. J. Packer, B. T. Pickup, and D. J. Wilton, J. Chem. Phys. **102**, 6128 (1995).
42. P.-O. Löwdin, Phys. Rev. **139**, 357 (1965).
43. R. McWeeny, *Methods of Molecular Quantum Mechanics* (Academic Press, London, 1989).
44. G. C. Wick, Phys. Rev. **80**, 268(1950); N. N. Bogoliubov and D. V. Shirkhov, Quantum Fields (Benjamin, Reading, MA, 1983).
45. L. S. Cederbaum, J. Chem. Phys. **62**, 2160 (1975).
46. (a) C. A. Coulson, Proc. Camb. Philos. Soc. Math. Phys. Sci., **36**, 201 (1940); (b) C. A. Coulson and M. S. Longuet-Higgins, Proc. R. Soc. A **191**, 39 (1947).
47. S. Wilson, in *Methods in Computational Molecular Physics*, S. Wilson and G. H. F. Diercksen, Eds. (Plenum, New York, 1992).
48. (a) N. M. Hugenholt, Physica **23**, 481 (1957); (b) L. Van Hove, N. M. Hugenholtz, and L. Howland, Quantum Theory of Many-Particle Systems (Benjamin, New York, 1961).
49. A. A. Abrikosov, L. P. Gorkov, and I. E. Dzyaloskind, *Methods of Quantum Field Theory in Statistical Physics* (Prentice Hall, Englewood Cliffs, NJ, 1963).
50. A. Szabo and N. S. Ostlund, *Modern Quantum Chemistry* (Macmillan, New York, 1982).
51. F. R. Harris, H. J. Monkhorst, and D. L. Freeman, *Algebraic and Diagrammatic Methods in Many-Fermion Theory* (Oxford University Press, Oxford, 1992).
52. P. Jørgensen and J. Simons, *Second Quantization-Based Methods in Quantum Chemistry* (Academic Press, New York, 1981).
53. See, e.g., (a) G. D. Purvis and Y. Öhrn, J. Chem. Phys. **60**, 4063 (1974); (b) G. Born, H. A. Kurtz, and Y. Öhrn, J. Chem. Phys. **68**, 74 (1978); (c) M. F. Herman, K. F. Freed, and D. L. Yeager, Adv. Quantum Chem. **48**, 1 (1981); (d) J. Baker, Chem. Phys. **79**, 117 (1983).